

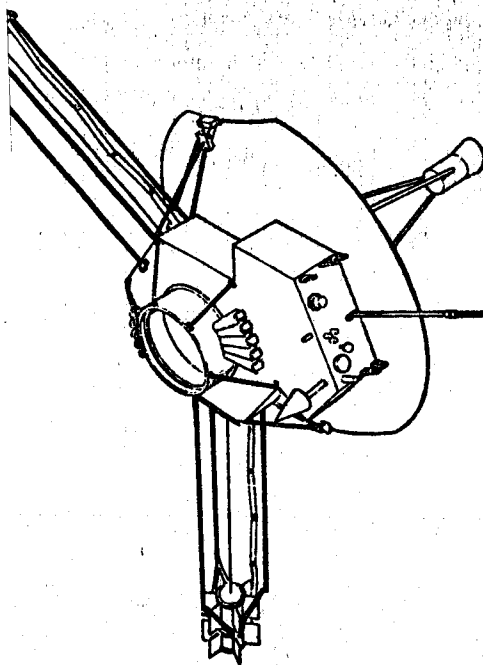
N80-72832

(NASA-CR-162891) PIONEER F AND G
SPACECRAFT/RTG REENTRY BREAKUP STUDY (TRW
Systems Group) 69 p

Unclas
15249

00/15

69 (PAGES)	DCAE (CODE)
CR-162891 (NASA CR OR TMX OR AD NUMBER)	(CATEGORY)
FF No. 602(A)	



TRW
SYSTEMS GROUP

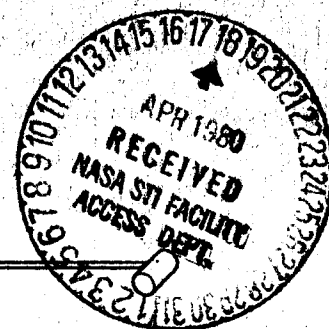
12356-6001-R0-00

PIONEER F & G SPACECRAFT/RTG REENTRY BREAKUP STUDY

JULY 28, 1970

Conducted for
NATIONAL AERONAUTICS
AND SPACE ADMINISTRATION
AMES RESEARCH CENTER

Contract NAS2-5222



12356-6001-RO-00

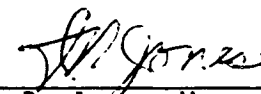
PIONEER F & G
SPACECRAFT/RTG
REENTRY BREAKUP STUDY

July 28, 1970

Compiled By:


J. M. Bell, Head
Nuclear Safety Section

Approved By:


I. R. Jones, Manager
Nuclear Systems Department

FOR
NATIONAL AERONAUTICS AND SPACE ADMINISTRATION
AMES RESEARCH CENTER

Contract NAS2-5222

TRW
SYSTEMS GROUP

CONTENTS

	Page
1. INTRODUCTION AND SUMMARY.	1-1
2. SPACECRAFT DESCRIPTION.	2-1
3. LAUNCH VEHICLE FAILURE MODES AND EFFECTS .	3-1
4. SPACECRAFT/RTG BREAKUP ANALYSIS	4-1
4.1 Random Orbital Decay	4-1
4.2 Prompt Reentry	4-19
5. PROPELLANT TANK FAILURE ANALYSIS.	5-1
5.1 Launch Pad Abort	5-1
5.2 High Altitude Abort	5-5
6. REFERENCES.	6-1

APPENDICES

A	NOMENCLATURE	A-1
B	STRUCTURAL ANALYSIS.	B-1

1. INTRODUCTION AND SUMMARY

The Pioneer F and G spacecraft, due to be launched in 1972 and 1973, respectively, will supply precursory scientific information beyond the orbit of Mars. The launch vehicle will be the Atlas/Centaur/TE 364-4 configuration. Spacecraft electrical power will be supplied by four radioisotope thermoelectric generators (RTGs). Current aerospace nuclear safety criteria require that the RTGs of the Pioneer F and G spacecraft be designed to preclude isotopic fuel release in all normal and accident environments. The responsibility for assuring that the RTGs meet these criteria rests primarily with the AEC and the RTG contractor. However, NASA Ames Research Center with responsibility for the Pioneer spacecraft, is responsible for determining the extent of any environments that may be imposed on the RTGs by the spacecraft in order that these environments may be considered in the RTG safety analysis.

The primary purpose of the study presented herein was to determine the conditions under which the RTGs or nuclear heat sources of the Pioneer F and G spacecraft become separated from the spacecraft during reentries resulting from two types of potential launch vehicle malfunctions. The secondary purpose was to define the environments imposed on the RTGs as the result of a spacecraft propellant tank rupture. This study was performed for NASA Ames Research Center under Contract NAS 2-5222.

The reentry breakup analyses considered two cases. Case 1 represented a launch vehicle malfunction in which the Centaur stage successfully fires, but some malfunction after firing prevents spin-up, TE 364-4 separation and ignition. That is, the Centaur/TE 364-4/spacecraft configuration is completely passive and the configuration undergoes random orbital decay. The results of the breakup analysis indicated that the RTG pairs would separate, intact, from the spacecraft at an altitude between 347,000 ft. and 355,000 ft., corresponding to trimmed and tumbling reentry modes, respectively. RTG release was found to be caused by melting of the RTG Support Trusses. Thermal analysis of the TE 364-4 motor indicated that auto-ignition of the propellant would not occur prior to RTG separation.

Case 2 represented a malfunction in which the TE 364-4 is misoriented

50 degrees from nominal at the time of ignition, which results in super-orbital reentry of the TE 364-4/spacecraft configuration. For this case, breakup was found to occur at 291,000 ft. and 271,000 ft., corresponding to trimmed and tumbling reentry modes, respectively. In this reentry case, the RTG pairs were found to be released, intact, from the spacecraft because of structural failure of the RTG Support Trusses.

Attitude misorientations of the TE 364-4 in the pitch plane result in the most severe reentry environments possible during the mission. Pitch (down) attitude misorientations of less than 50 degrees may result in grazing reentry, multiple skips, or even escape. Because of the difference in ballistic coefficient between the RTGs and the spacecraft, and the conditions under which the spacecraft releases the RTGs, the reentry conditions required to result in the various reentry trajectories, and the effects of these reentries on the RTGs, will vary appreciably. Therefore, it is recommended that further analyses be conducted to determine the release conditions, and the initial reentry conditions, which will cause the RTGs subsequently to be exposed to the grazing reentry, multiple skip, or escape. The results of these analyses will subsequently allow appraisal of the effects of these reentry conditions on the RTGs.

2. SPACECRAFT DESCRIPTION

The Pioneer F and G spacecraft, designed for flyby missions of Jupiter, are scheduled for launch during 1972 and 1973. The spacecraft weighs about 550 pounds and is spin stabilized with the spin axis pointing toward the earth. The spin axis is offset from the center but parallel to the large 9-foot diameter antenna which provides high bit rate from Jupiter. On two of the three booms (see Figure 2-1) are mounted two modified SNAP-19 radioisotope thermoelectric generators (RTGs). These RTGs are deployed (on long thin tubes) to reduce radiation and magnetic interference and are oriented such that the shadow angles minimize interference with the radiation experiment sensors. The third boom separates the flux gate magnetometer 20 feet from the spacecraft. The boom uses a viscous damper to rapidly remove any wobble induced by spacecraft maneuvering.

The sensor compartment is thermally isolated from the sun and uses heat released by the equipment, in particular the 8-watt TWT's, to maintain a satisfactory thermal environment for all of the spacecraft and scientific equipment. While the spacecraft is generally thermally independent of the sun when it is near the earth just after launch, a temporary condition of high internal heat could arise. For this reason a bank of thermal louvers is mounted just outside of the interstage range.

At the apex of the tripod of the high-gain antenna is the antenna feed. Above this is a medium-gain antenna which is pointed off axis and used for communication near the earth and for attitude acquisition by conically scanning the S-band signal from the earth. The spacecraft is torqued by a hydrazine gas system whose jets are located at opposite positions near the rim of the large antenna. The signal from the earth is first nulled on the medium-gain antenna and secondly on the high-gain antenna, which has a movable feed to provide a beam offset during the conical scan maneuver.

The hydrazine system used for both spacecraft orientation and for midcourse propulsion has a 16.5-inch tank which is used in a simple blowdown mode; there are about 60 pounds of propellant of which 2 pounds

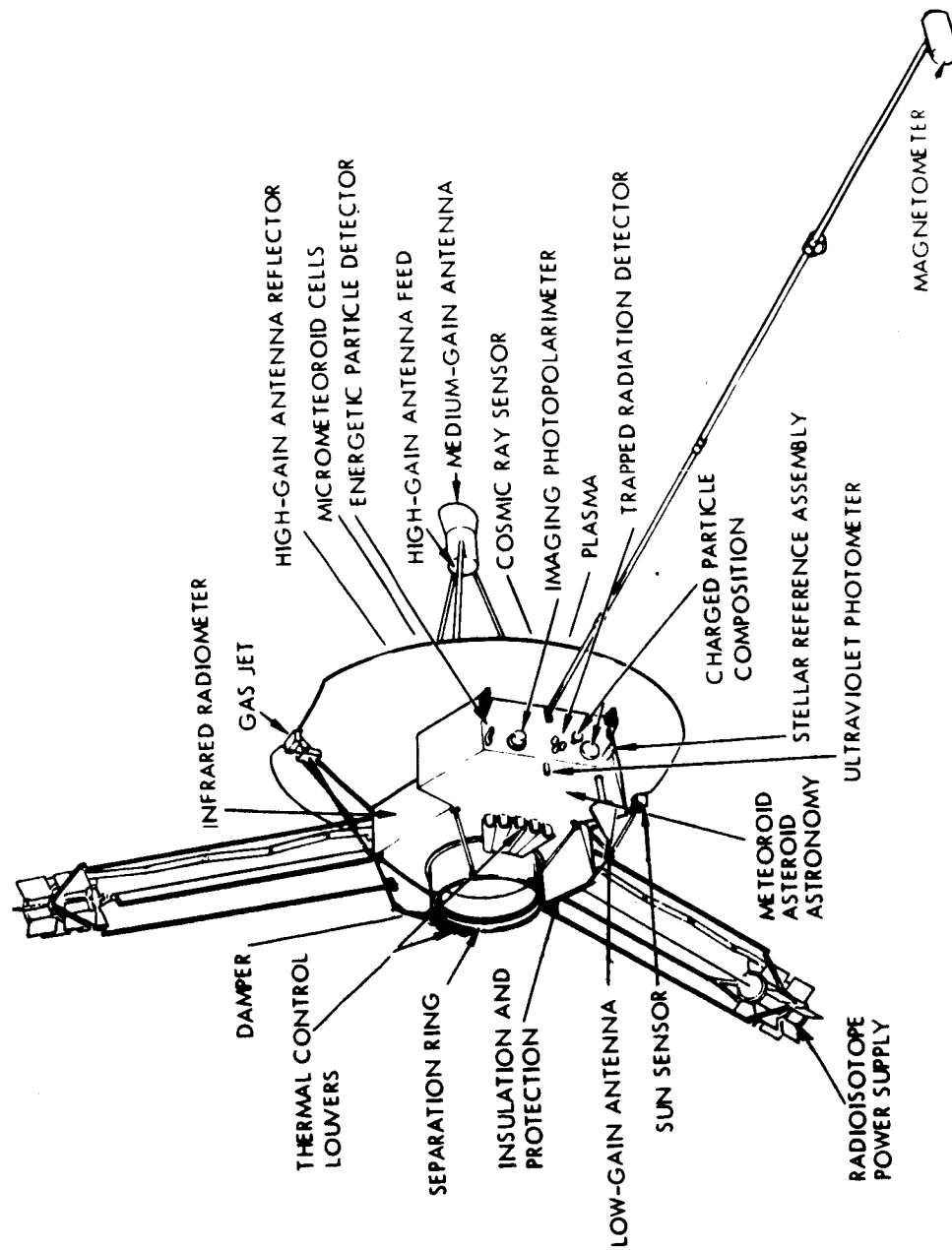


Figure 2-1. Pioneer F and G Spacecraft

are required for spin control and despin of the spacecraft after injection from the spin-stabilized TE 364-4 stage, eight pounds for attitude pointing and orientation maneuvers, and the remainder available for midcourse ΔV . This system has an I_{sp} in the ΔV mode of about 215 seconds. It can be used in pulsewidths of about 31, 100, 500, and 1000 milliseconds. These pulsewidths provide adequate step size for rapid acquisition of the spacecraft to the earth and small step sizes for maintaining good pointing accuracy. The beamwidth of the high-gain antenna is about ± 2 degrees. Therefore, the spacecraft must be torqued at regular intervals to keep the earth in the center of that beam. Torquing updates of the pointing attitude are required on the order of two or three times a day during the early stages of the mission but only four or five times a month after Jupiter. The system is also used to torque the spacecraft to a proper attitude for a midcourse correction and the engines are fired in couples for the midcourse correction itself. Over 200 m/sec are available for this correction.

A high-gain antenna of about 32 db gain is used with an 8-watt tube at S-band and can provide 1024 bps at 6 AU, the maximum Jupiter range. The medium-gain antenna used for uplink communications in the conical scan mode can ensure that the spacecraft is in the middle of the high-gain antenna out to 20 AU with a 3-db margin with the 210-foot ground antennas and 40-kw transmitters. A low-gain rearward facing antenna provides communication during the injection and orientation after launch. A sun sensor supplies the signal to drive the spacecraft around into the direction of the sun and provide sun pulses. Finally, as can be seen in Figure 2-1, a stellar reference assembly is provided which measures pips from the star Canopus and determines spin rate.

The four SNAP 19 RTGs each provide about 50 watts of power at the beginning of mission life and about 30 watts at the end of eight years. This extended life estimate awaits verification since there are not adequate test data. If correct, the 120 watts at the end of eight years more than meets the current Pioneer F and G requirement of 107 watts of which 24 watts are required for the science payload.

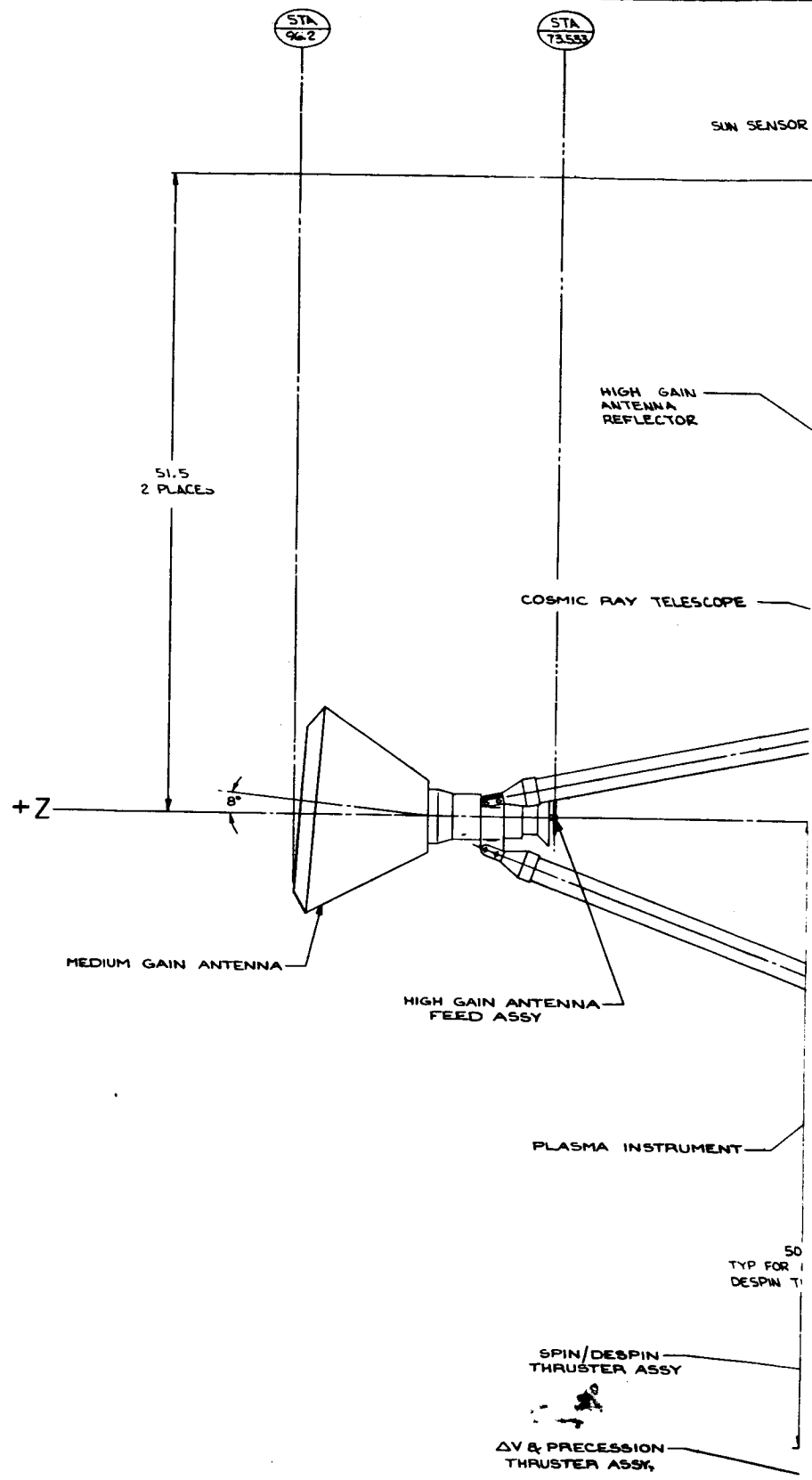
Table 2-1 summarizes the properties of the major spacecraft components, and Figures 2-2 through 2-5 show the details* of the spacecraft construction, experiments, and RTG attachments.

*Subject to change.

Table 2-1. Major Pioneer Spacecraft Components

Component	Approximate Size (Inches)	Approximate Weight (Pounds)	Material
<u>ANTENNA</u> Feedhorn Assembly (Medium Gain) Reflector Assembly	18 Diameter 10 Long	3.8	Sheet Metal (Aluminum)
	108 Diameter	24.2	Adhesive Bonded 0.004" Thick Sheeting Over 0.625" Thick Honeycomb Core (Aluminum)
	1.26 Diameter 61.1 Long	.7 Each	Boron Circumferentially Wrapped Filament
<u>EQUIPMENT BAY</u> Platform Side Panels and Interior Bulkhead (11) Cover Panels (4)	61.54 Long ~50 Wide	17.2	0.16 Aluminum Sheets Over 0.782 ³ Honeycomb Core (3.1 pound per Ft ³)
	13 x 24	11.0	0.010 Aluminum Sheets Over 0.500 Honeycomb Core
		7.3	
<u>PROPELLANT TANK</u> (including Support Structure)	16.6 Diameter	10.9 (empty)	Titanium Alloy (0.034 In Thick Walls)
<u>RTG GUIDE RODS</u> (6)	73.5 Long	.4 each	.625 Diameter Aluminum Tube .028 Wall Thickness
<u>ADAPTER</u> (Spacecraft/Inter- stage assembly)	25.09 Diameter 6.25 Long	13.6	Fiberglass (0.090 Wall Thickness)
<u>INSULATION</u>	.0115 Thick	6.9	22 Layers 0.00025 Kapton Plus Two Layers .003 Thick

	16	15	14
H	<div> <p>THE INFORMATION AND TECHNICAL DATA DISCLOSED BY THIS DOCUMENT MAY BE USED WITHOUT RESTRICTION BY AND FOR THE UNITED STATES GOVERNMENT OR BY ANY PERSON OR ORGANIZATION CONTRACTING WITH THE UNITED STATES GOVERNMENT, EXCEPT WHERE A LIMITED P. ARTS LICENSE FOR ADP'S ALSO APPEARS ON THIS DOCUMENT, AND MAY BE USED BY OTHERS OUTSIDE OF THE SYSTEM WHERE RIGHTS ARE EXPRESSLY GRANTED BY A TWO SYSTEM CONTRACT. EXCEPT AS NOTED ABOVE, THE INFORMATION AND TECHNICAL DATA DISCLOSED BY THIS DOCUMENT ARE PROPRIETARY TO THE SYSTEM AND MAY BE USED, REPRODUCED, OR DISSEMINATED IN ANY MANNER EXCEPT WHERE NECESSARY TO COMPLY WITH A TWO SYSTEM CONTRACT OR AS AUTHORIZED BY THE SYSTEM.</p> </div>		
G			
F			
E			
D			
C			
B			
A			
	16	15	14



50
TYP FOR
DESPIN T

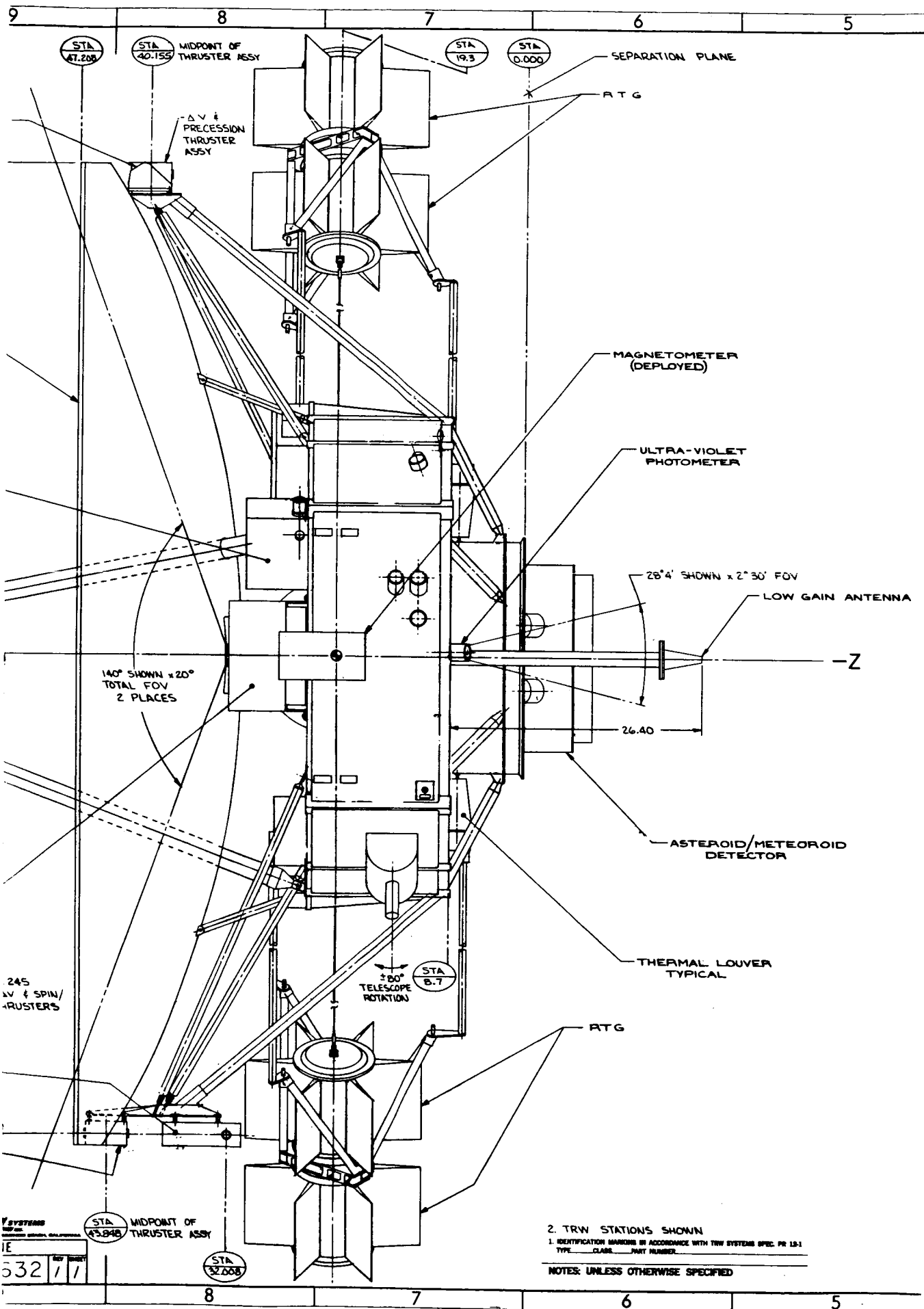
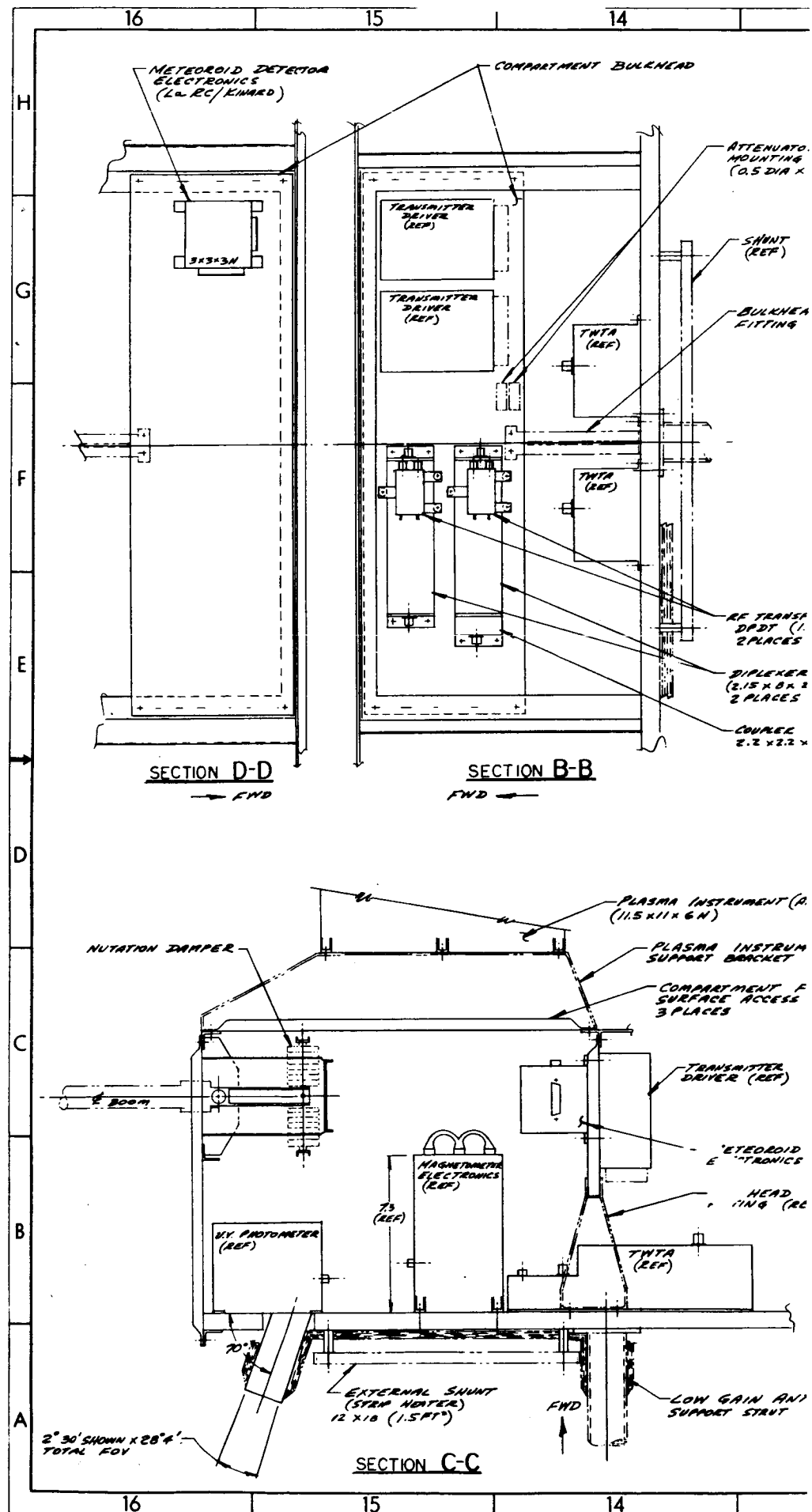
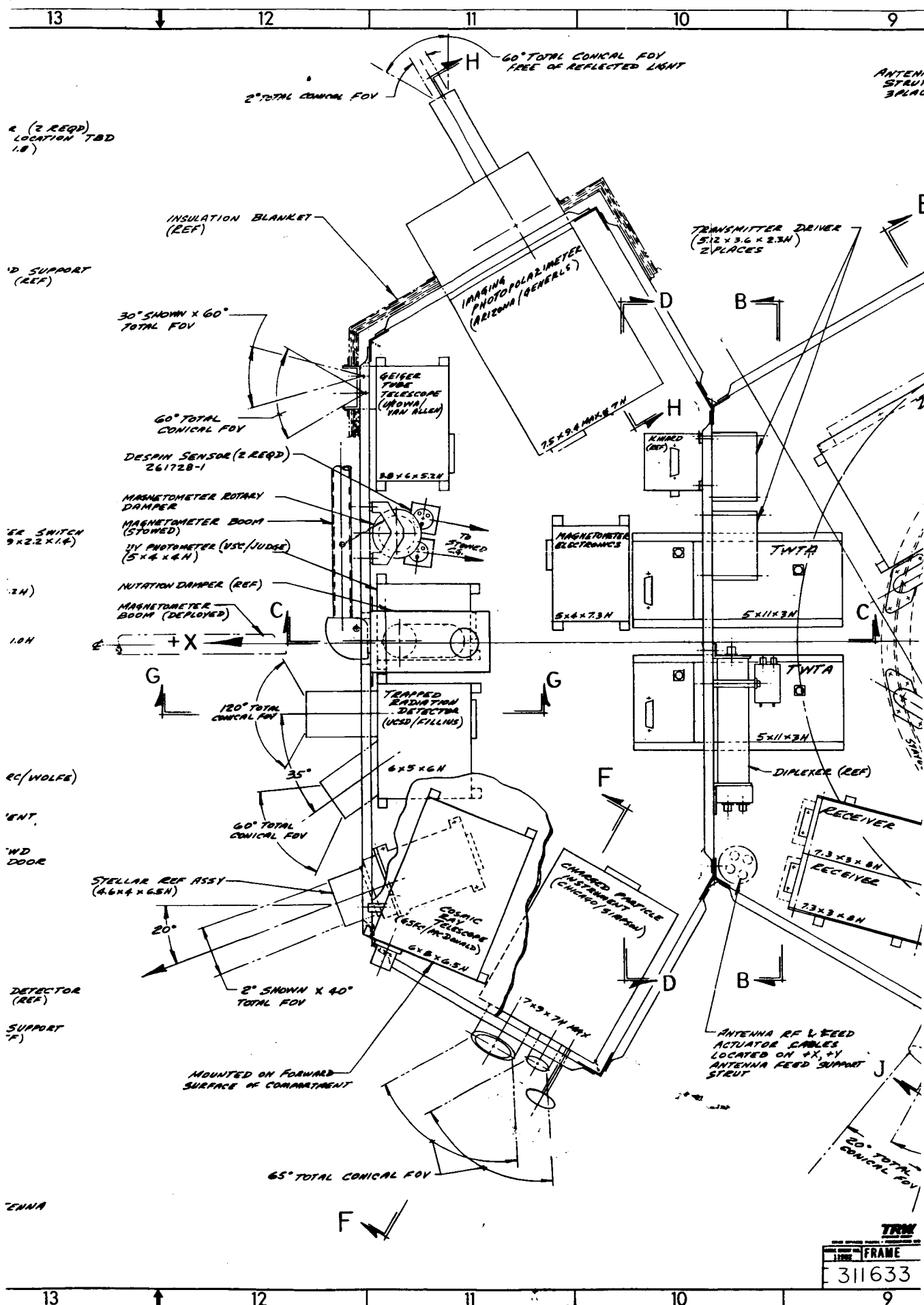
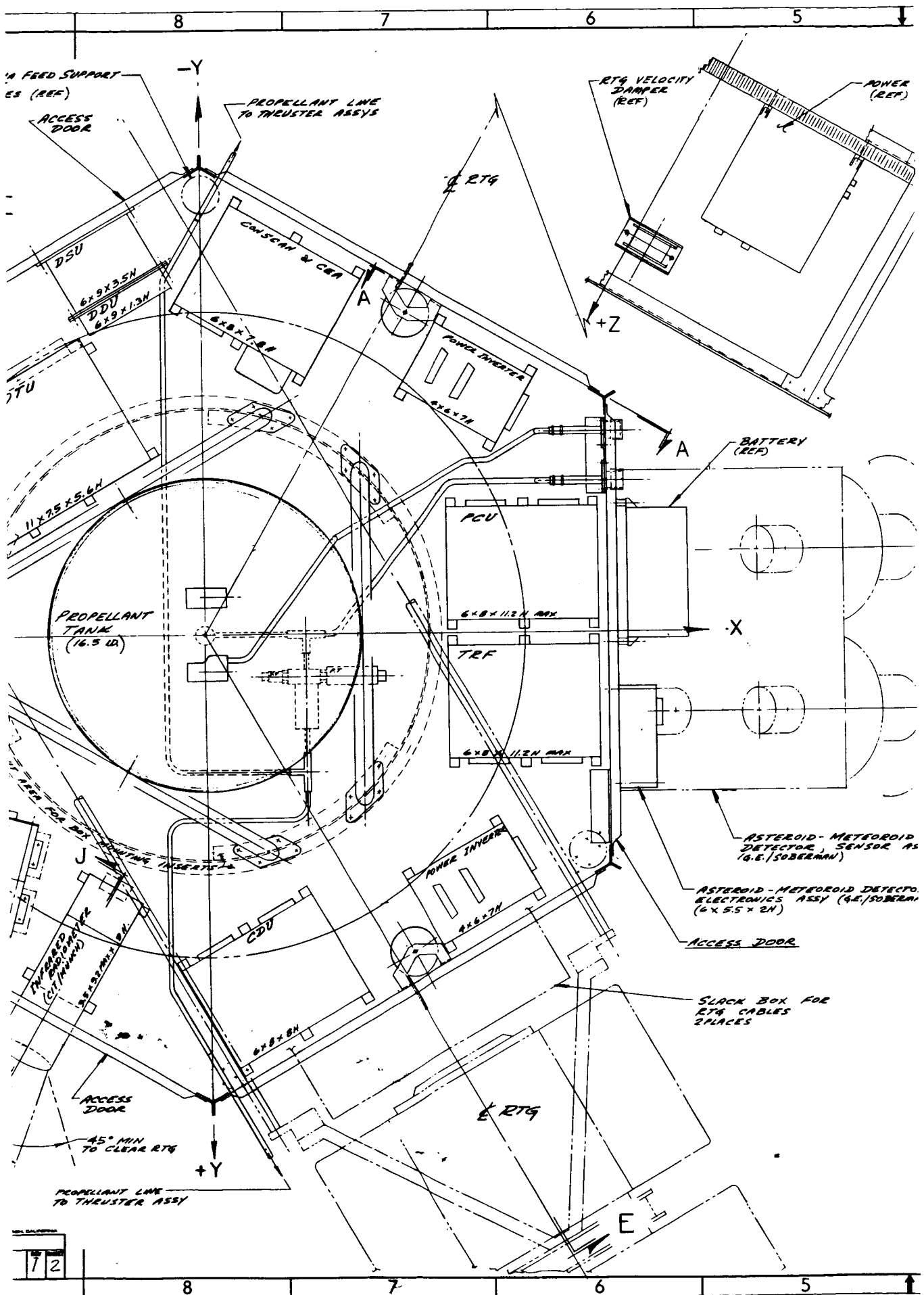


Figure 2-2. Spacecraft External Configuration







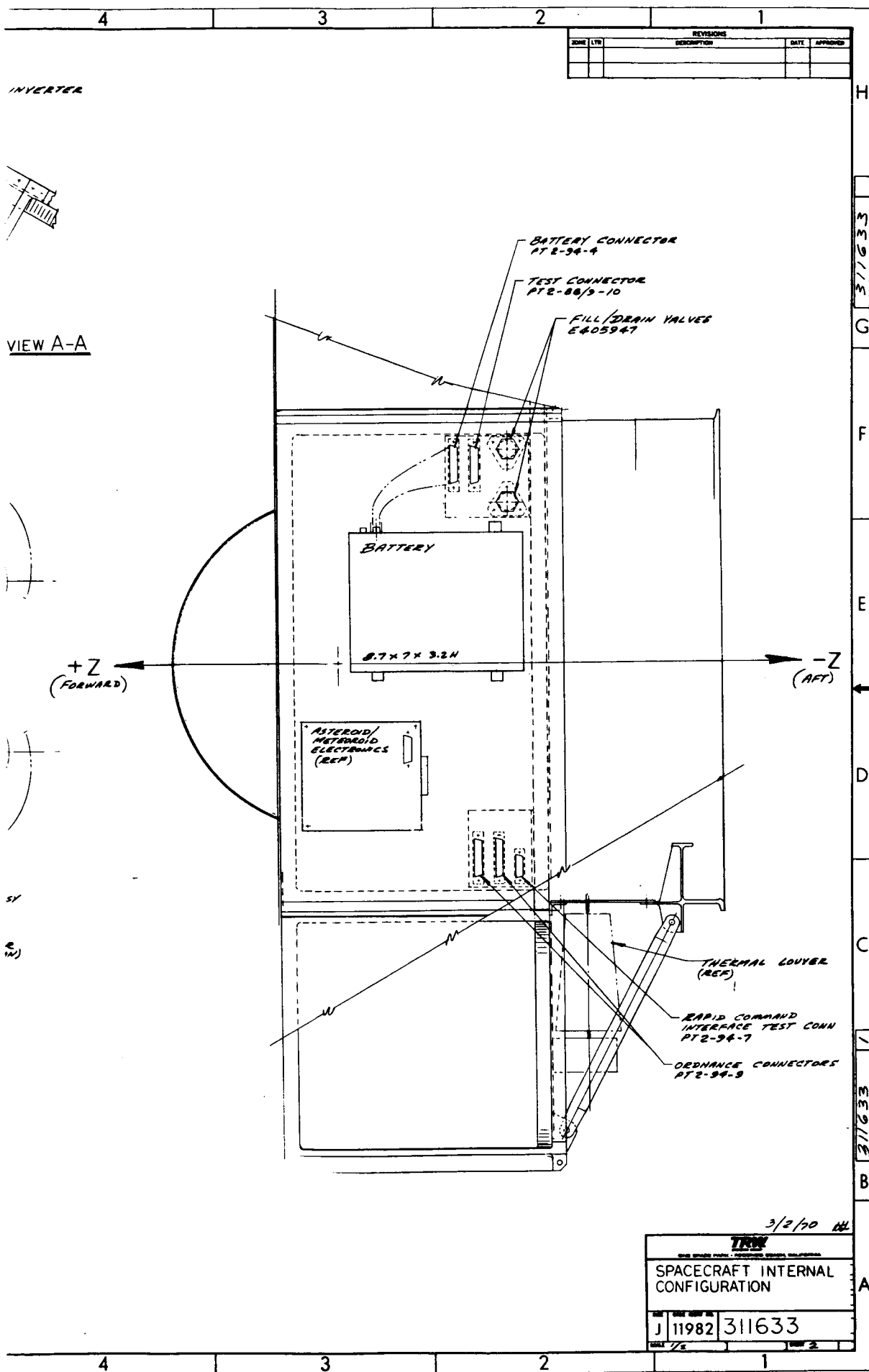
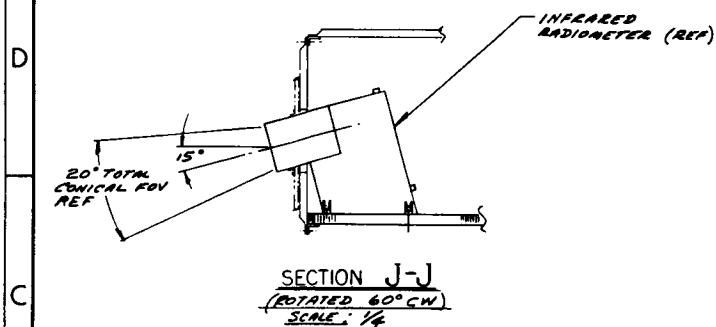
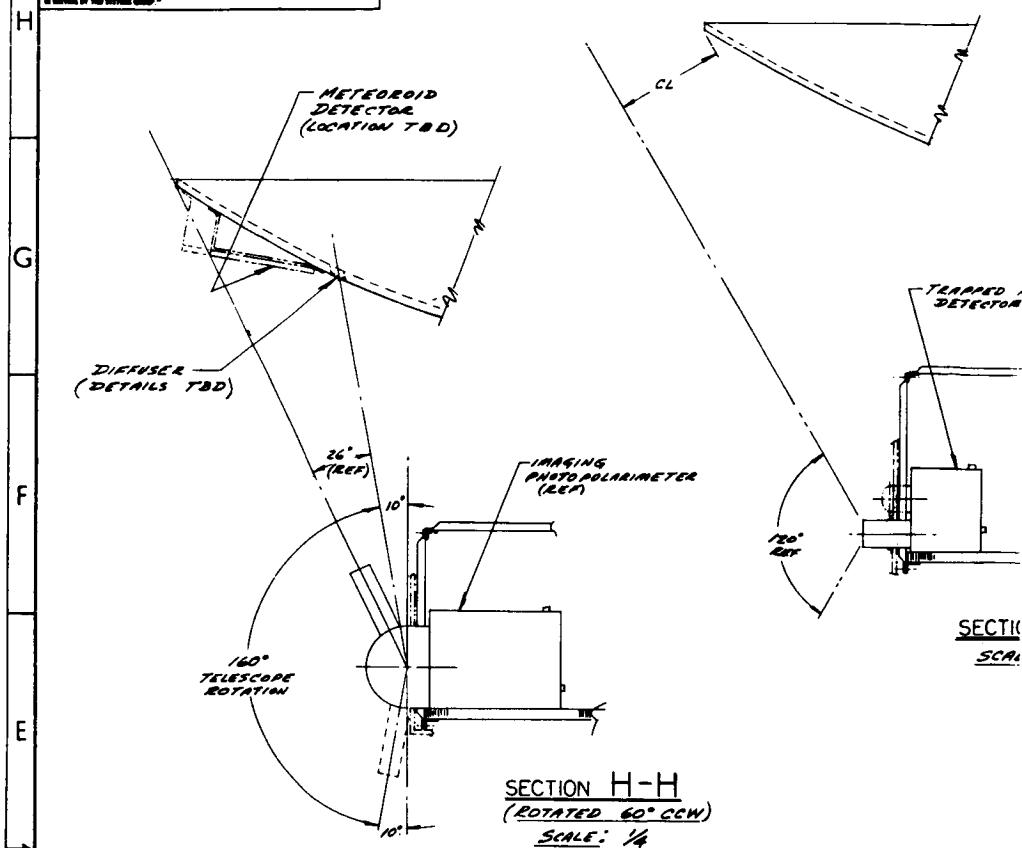
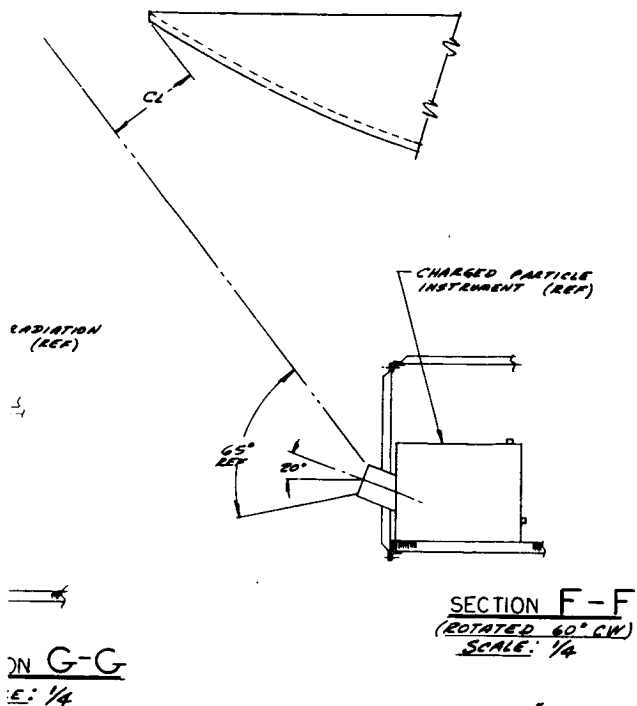


Figure 2-3. Spacecraft Internal Configuration (Top View)

"THE INFORMATION AND TECHNICAL DATA DISCLOSED BY THIS DOCUMENT IS THE PROPERTY OF THE GOVERNMENT OF THE UNITED STATES OF AMERICA AND IS NOT TO BE REPRODUCED OR TRANSMITTED IN ANY FORM OR BY ANY MEANS, ELECTRONIC OR MECHANICAL, INCLUDING PHOTOCOPYING, RECORDING, OR BY ANY INFORMATION STORAGE AND RETRIEVAL SYSTEM, WITHOUT PERMISSION IN WRITING FROM THE GOVERNMENT OF THE UNITED STATES OF AMERICA."





HIGH GAIN ANTENNA REFLECTOR
SUPPORT STRUTS - 12 PLACES

THERMAL INSULATION
BLANKET (REF)

DDU
(REF)

DSU
(REF)

DTU
(REF)

PROPELLANT TANK ASSY
(16.5 I.D.)

THERMAL LOUVER ASSY
(REF)

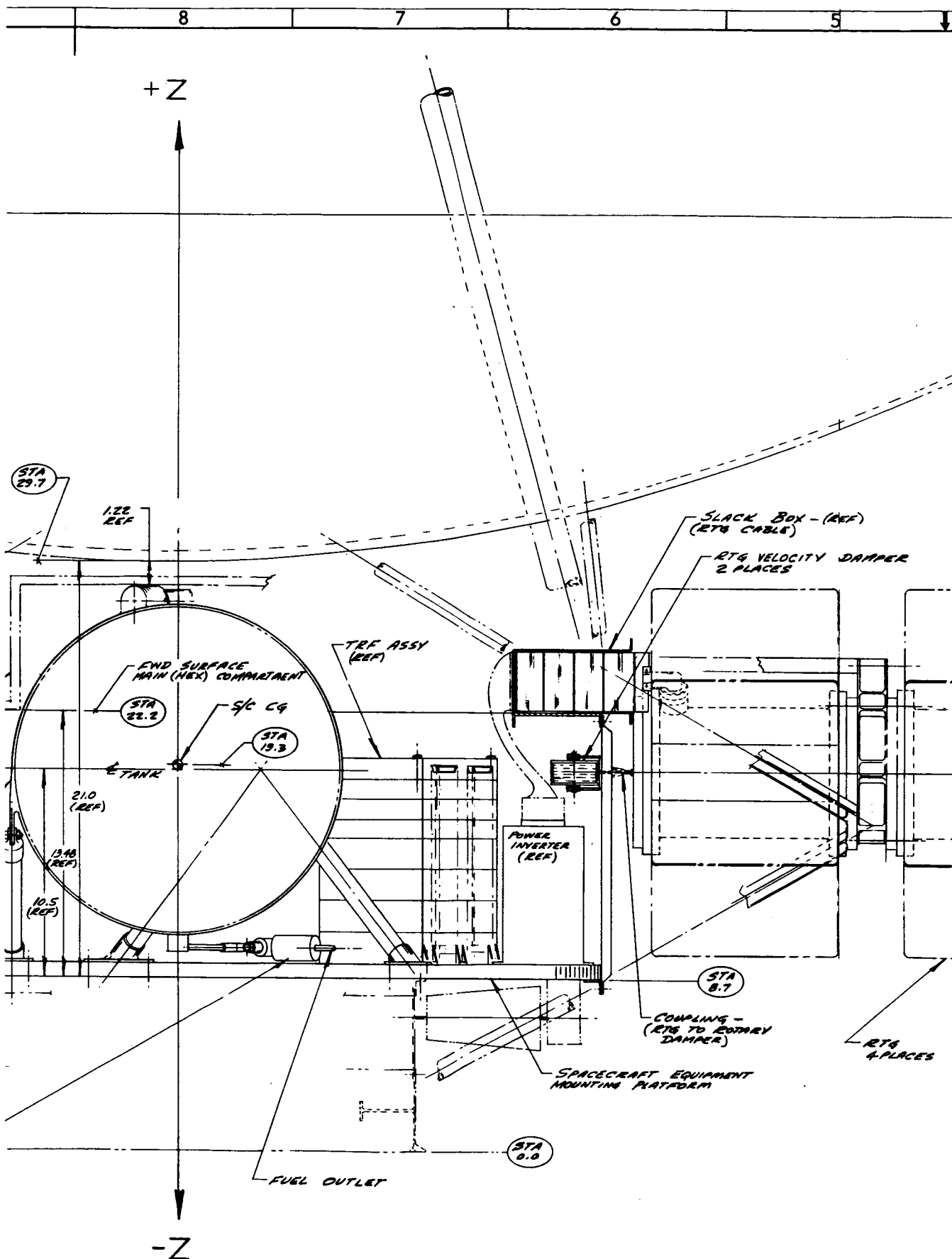
INTERSTAGE SUPPORT
STRUT, 6 PLACES

S/C INTERSTAGE ASSY

PROPELLANT FILTER
ASSY

HIGH & MEDIUM GAIN
FEED SUPPORT STRUT
3 PLACES

STA
19.2

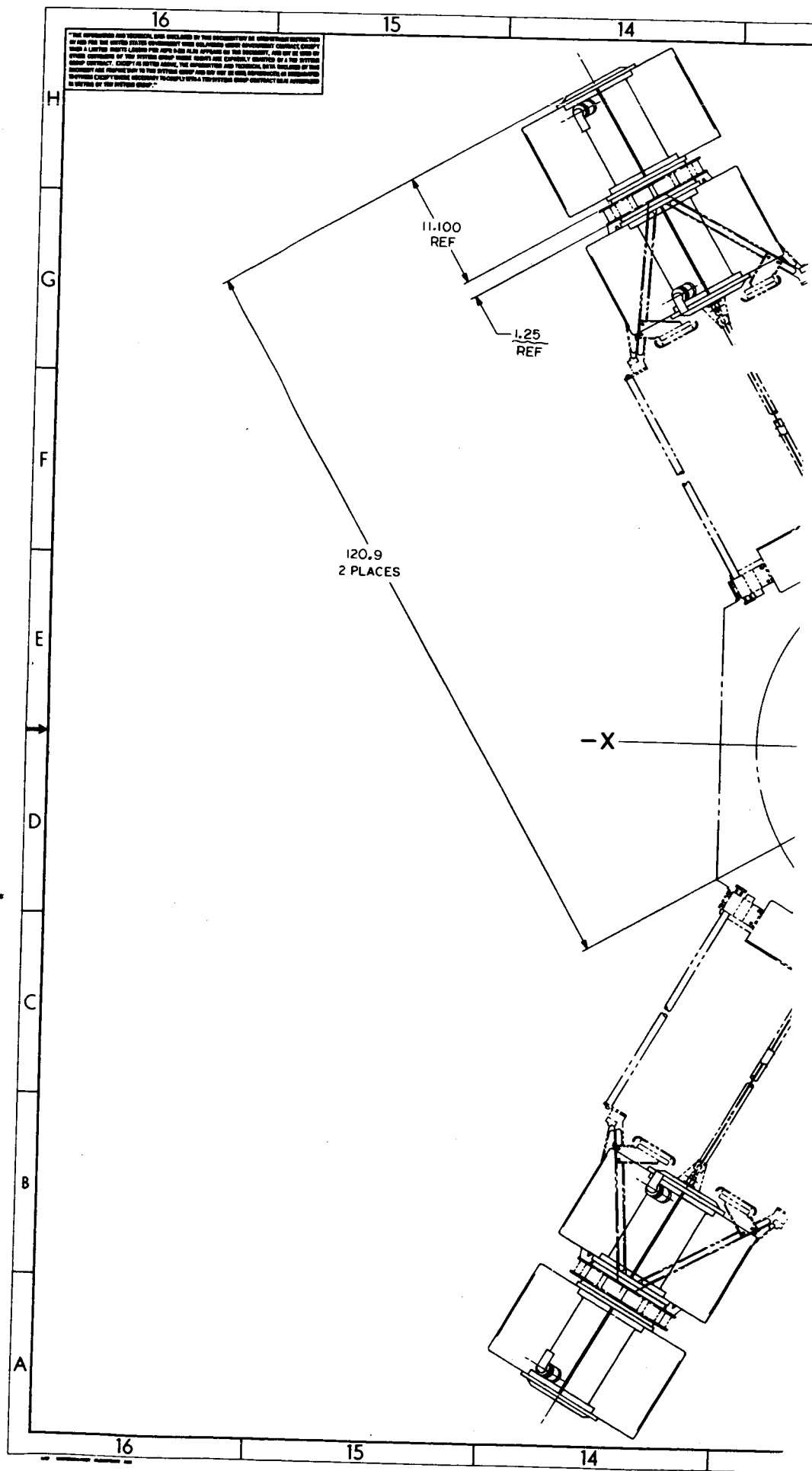


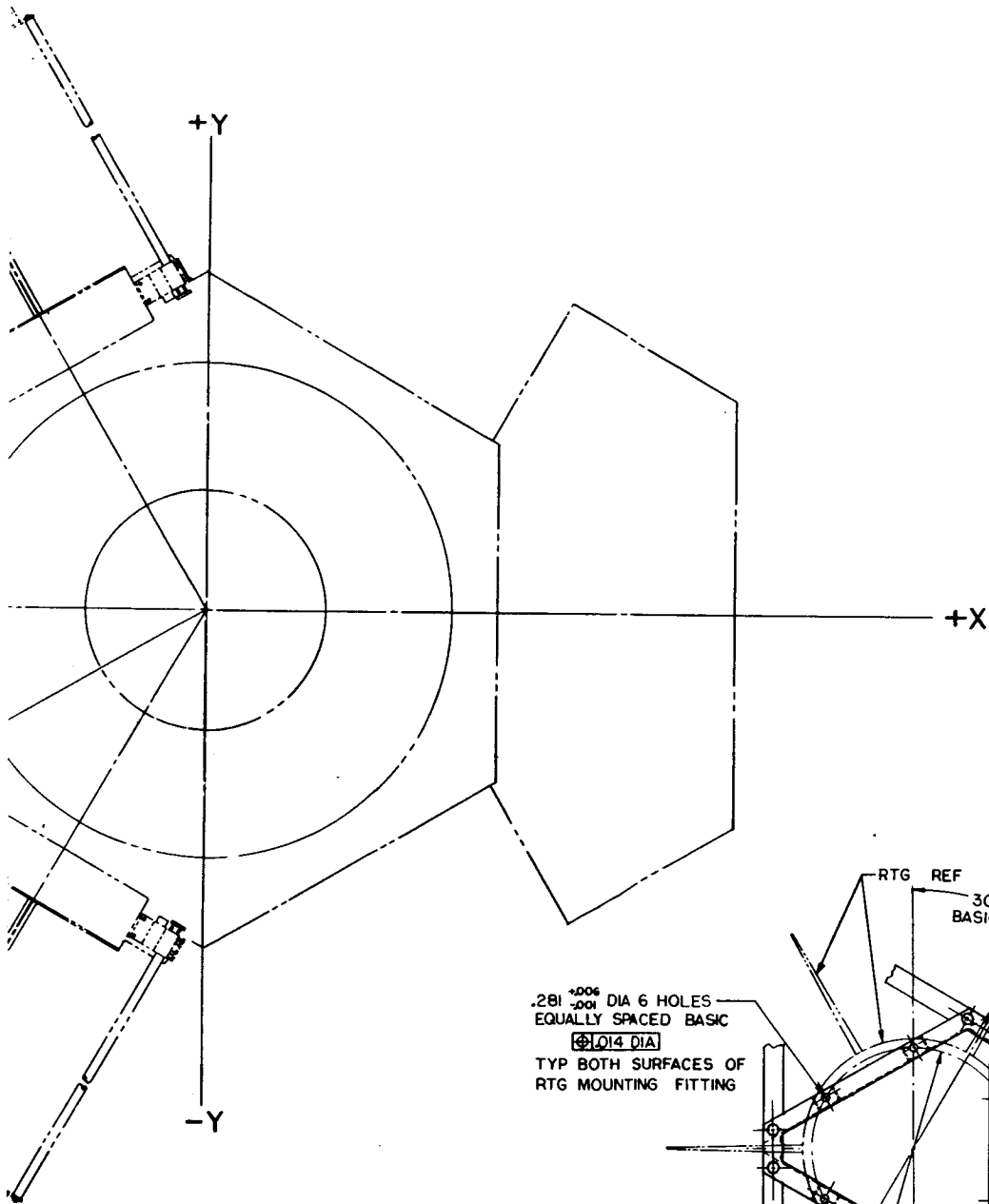
SECTION **E E**
(ROTATED 60° CCW)

9/4
SHR

1. IDENTIFICATION NUMBER PER FIG 12-1
TYPE _____ CLASS _____ PART NUMBER _____

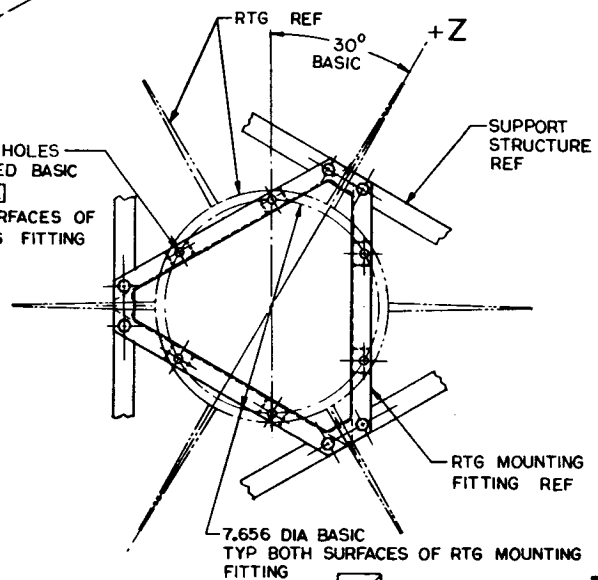
NOTES: UNLESS OTHERWISE SPECIFIED





RTG's DEPLOYED
VIEW LOOKING AFT

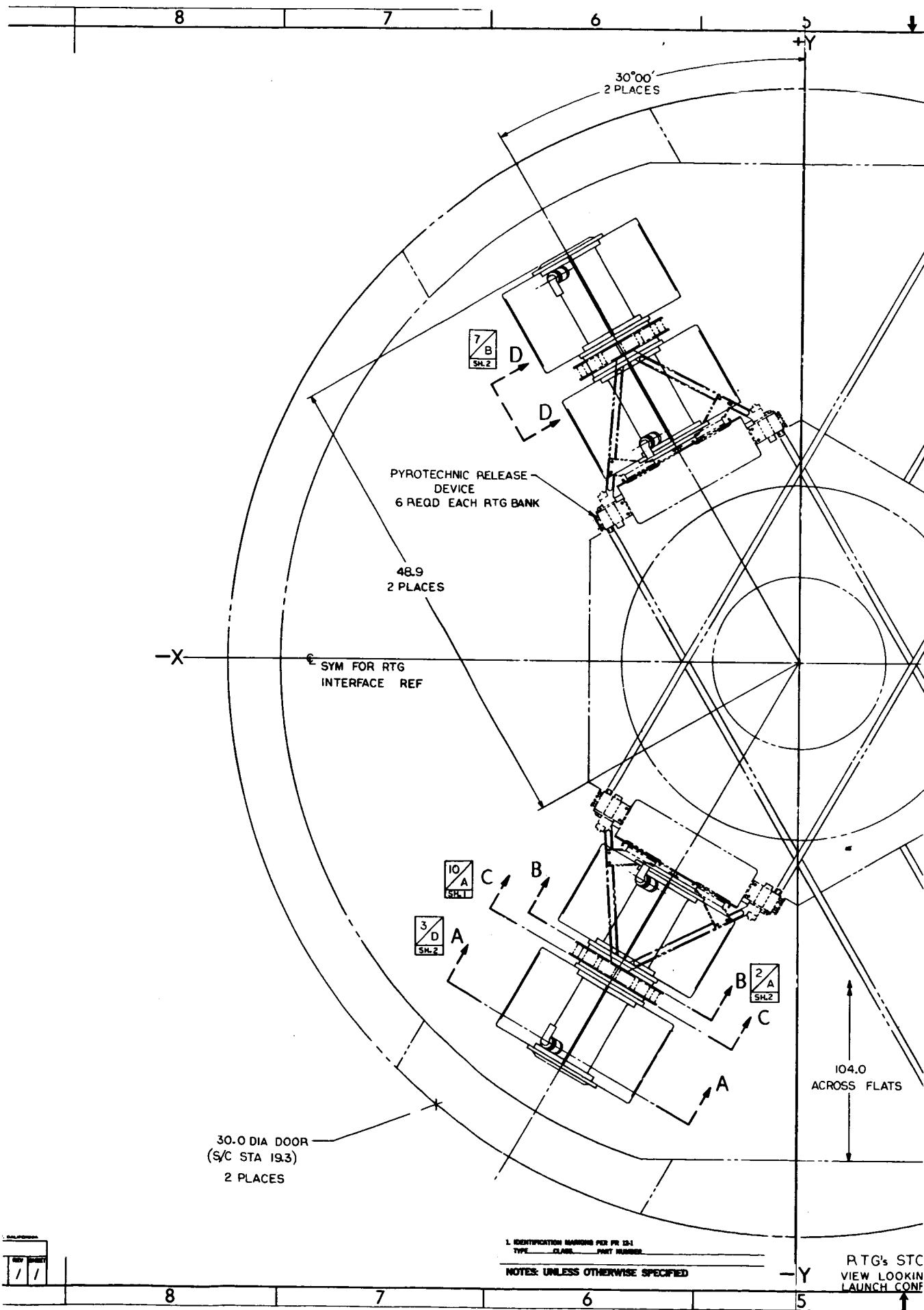
.281 $\pm .006$ DIA 6 HOLES
EQUALLY SPACED BASIC
Ø.014 DIA
TYP BOTH SURFACES OF
RTG MOUNTING FITTING



SECTION C-C
SCALE 1/2
SIMILAR 2 PLACES



TRW
11/82 FRAME
C311635



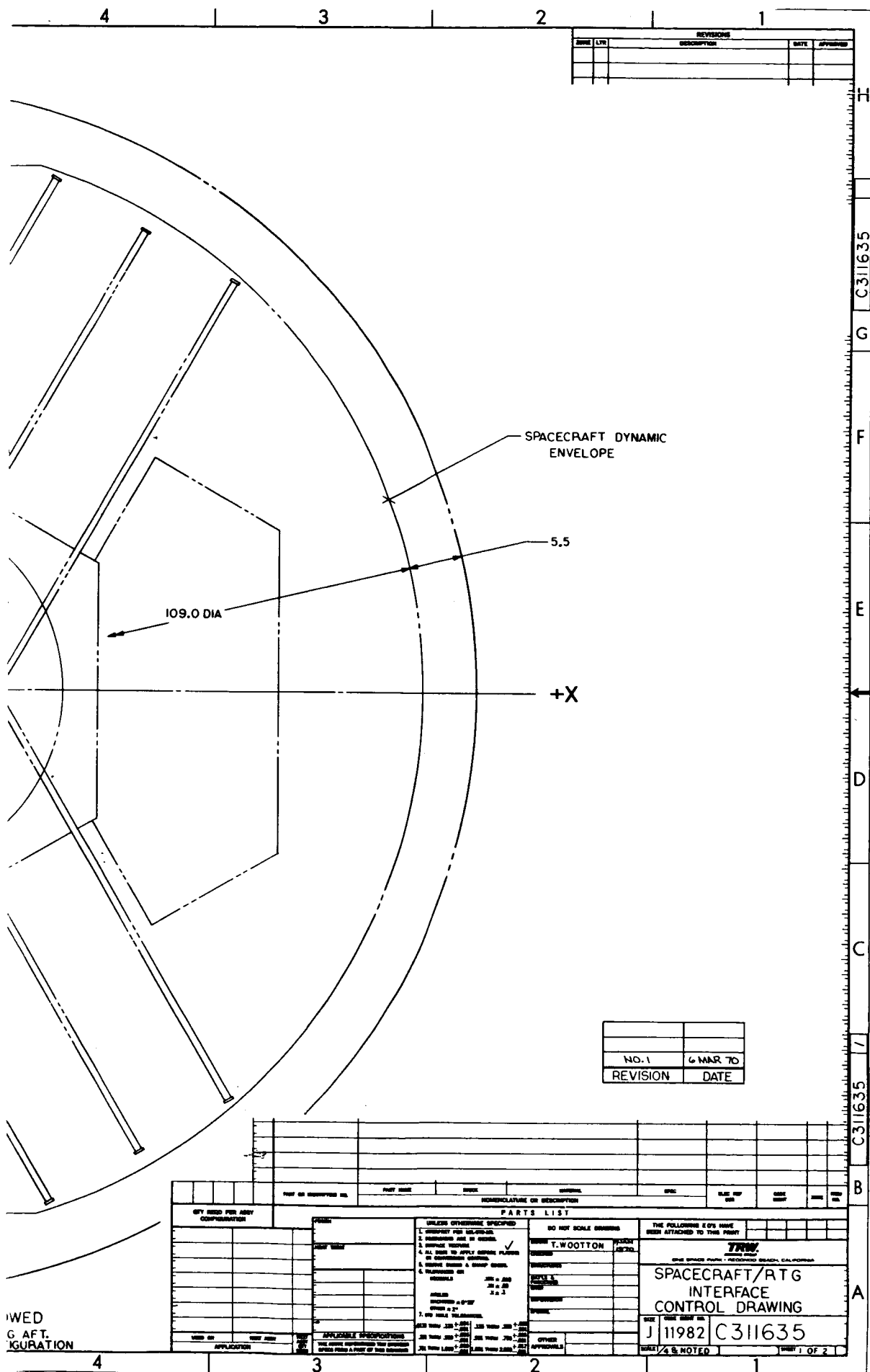


Figure 2-5. Spacecraft/RTG Interface
2-8

3. LAUNCH VEHICLE FAILURE MODES AND EFFECTS

A preliminary investigation was conducted into potential launch vehicle failures in order to identify the configurations that could reenter after a high altitude abort. The investigation was based on the conservative assumption that, although range safety destruct action can be taken at any time up until the end of the Centaur coast phase, destruct action would not be taken. The second assumption that was made was that only single failures occurred. The investigation was meant to provide a 'first look' at the various possibilities, rather than a comprehensive review.

The results are shown in Table 3-1. The first column identifies the types of failures that may occur, based on the nominal sequence of events. The second column identifies typical potential causes of these failures. The immediate effects of the failure are listed in the third column. The fourth column describes the immediate, orbital configurations. The potential trajectories arising from each failure are shown in the fifth column, where 'Escape' implies that the resultant configuration may dip into the atmosphere, but under such conditions that it subsequently escapes the earth's gravitational field. Finally, the initial reentry configurations are listed in the sixth column for those failures and trajectories which result in immediate or eventual reentry.

Failure 1 represents a random orbital decay of the Centaur (empty)/TE 364-4 (full)/spacecraft configuration. Because it is assumed that the Centaur flight programmer fails, the spacecraft is not separated from the TE 364-4, and the RTG deployment timer, therefore, is never activated. Thus the RTGs remain undeployed. A reentry breakup analysis of Failure 1 is contained in Section 4-1.

Failure 2 results in a TE 634-4 spin speed which is less than the nominal. Depending on what the actual spin speed is, a hard-over tumble or gross or minor coning motion may result from the TE 364-4 burn. Because of the spiralling motion that occurs during a hard-over tumble, the resultant velocity vector after the TE 364-4 burn may be essentially equal to the velocity vector prior to ignition, such that the configuration remains in orbit for a time prior to orbital decay reentry. As shown

Table 3-1. Failure Modes and Reentry Configurations (Single Failures Only)

FAILURE	POTENTIAL CAUSES	POTENTIAL EFFECTS	RESULTANT CONFIGURATIONS	TRAJECTORIES	INITIAL REENTRY CONFIGURATIONS
1. TO SPIN/SEPARATE/ THRUST	A. CENTAUR FLIGHT PROGRAMMER	1. PASSIVE VEHICLE	A. CENTAUR/3RD STAGE/S-C	1. R.O.D. (RANDOM ORBITAL DECAY)	A. CENTAUR (EMPTY)/TE 364-4 (FULL)/ S-C (BOOMS UNDEPLOYED).
2. TO ATTAIN SPIN SPEED (0 $\leq \omega < 60$ RPM)	A. CENTAUR FLIGHT PROGRAMMER (1ST DISCRETE); ONE OR MORE SPIN MOTORS	1. HARD-OVER TUMBLE	A. RTG'S SEPARATED FROM S-C B. S-C SEPARATED FROM TE 364-4 C. TE 364-4/S-C INTACT	1. R.O.D. (1) 1. R.O.D. (1) 1. R.O.D. (1)	A. RTG'S (5) A. S-C (BOOMS DEPLOYED) (2) B. S-C (BOOMS UNDEPLOYED) (3) A. S-C (BOOMS DEPLOYED) (2) B. S-C (BOOMS UNDEPLOYED) (3) A. S-C (BOOMS DEPLOYED) (2) B. S-C (BOOMS UNDEPLOYED) (3)
3. TO SEPARATE CENTAUR/ TE 364-4	A. CENTAUR FLIGHT PROGRAMMER (2ND DISCRETE); MARMON CLAMP MALFUNCTION	1. HARD-OVER TUMBLE 2. CONING	A. TE 364-4/S-C INTACT (4) SAME AS ABOVE SAME AS ABOVE	1. ESCAPE 2. R.O.D.	A. S-C (BOOMS DEPLOYED) (2) B. S-C (BOOMS UNDEPLOYED) (3)
4. TO RETRO CENTAUR	A. CENTAUR FLIGHT PROGRAMMER; INSUFFICIENT RESIDUAL GAS; PNEUMATIC SYSTEM MALFUNCTION	VARIOUS			
5. TO IGNITE TE 364-4	A. CENTAUR FLIGHT PROGRAMMER (1ST DISCRETE); FUSE; MOTOR	1. ESCAPE TRAJECTORY NOT OBTAINED	A. S-C (BOOMS DEPLOYED)	1. R.O.D.	A. S-C (BOOMS DEPLOYED)
6. TO ACHIEVE DESIRED ALTITUDE AT TE 364-4 IGNITION	A. CENTAUR GUIDANCE OR CONTROL SYSTEM FAILURE	1. INCORRECT TRAJECTORY	A. ANY	1. ESCAPE 2. R.O.D. 3. GRAZE 4. SKIP 5. PROMPT	A. S-C (BOOMS DEPLOYED) A. CENTAUR (EMPTY)/S-C (BOOMS UNDEPLOYED) B. S-C (BOOMS UNDEPLOYED) C. S-C (BOOMS DEPLOYED) SAME AS GRAZE - A, B, C SAME AS GRAZE - A, B, C A. S-C (BOOMS DEPLOYED)
7. TO ATTAIN ESCAPE VELOCITY	A. MOTOR PREMATURE THRUST TERMINATION; CASE BURN- THROUGH	1. ESCAPE TRAJECTORY NOT ATTAINED	A. S-C (BOOMS DEPLOYED)	1. R.O.D.	

- (1) MOST PROBABLE TRAJECTORY
(2) $\omega > 40$ RPM (APPROX.)
(3) $\omega < 40$ RPM (APPROX.)
(4) MOST PROBABLE CONFIG.
(5) SINGLE RTG, PART OF RTGS, OR PART OF RTGS
WITH RTG SUPPORT TRUSS ATTACHED.

in the sixth column, this tumbling motion may cause the RTGs to separate from the spacecraft because of the centrifugal forces produced on the collar between each RTG in a pair, and on the truss which supports each pair of RTGs. If, instead, the spacecraft is detached at the TE 364-4/spacecraft interface because of centrifugal forces, the RTGs and magnetometer booms may or may not be deployed prior to reentry, depending on the spin speed. The despin sensor assembly on the spacecraft will prevent boom deployment if the spin speed is less than approximately 40 rpm. If, after the hard-over tumble, the TE 364-4/spacecraft is intact and assuming TE 364-4/spacecraft separation later occurs automatically, the booms may or may not be deployed at reentry, again depending on the spin speed. If coning rather than a hard over tumble, occurs as the result of a less than normal spin speed, it is anticipated that the TE 364-4/spacecraft would remain intact, in which case the configuration would probably escape or undergo random orbital decay, depending on the extent of the coning. Assuming normal, automatic separation of the spacecraft from the TE 364-4, the spacecraft could reenter with, or without, the booms deployed.

Failure 3 represents a case in which the spin-stabilized TE 364-4 ignites while still attached to the Centaur. It is anticipated that the results of this failure would be similar to those from Failure 2. An additional consideration in this case is that the residual propellants in the Centaur stage may be exploded by the exhaust from the TE 364-4.

Failure 4 is a case wherein the Centaur does not undergo the planned retromaneuver prior to TE 364-4 ignition. The potential effects probably range from zero perturbation to the mission, to explosion of the residual propellants in the Centaur stage.

In the event that the TE 364-4 failed to ignite, the spacecraft, with booms deployed, would reenter in an orbital decay made as shown in Failure 5.

Failure to achieve the desired attitude at TE 364-4 ignition could result in a spectrum of reentry configurations and trajectories, as indicated for Failure 6. The exact degree of pitch and/or yaw attitude misorientation determines the initial reentry conditions, the time to reentry, and therefore, the reentry configuration. A reentry breakup

analysis based on a prompt reentry of the TE 364-4 (empty)/spacecraft (booms undeployed) configuration is contained in Section 4.2.

From columns 7 and 8 of Figure 3-1, the range of potential reentry configurations and reentry modes is shown in Table 3-2. Not all of the combinations of configuration and reentry mode result in severe reentry conditions. For example, of the grazing reentries, the configuration shown as (7) is associated with higher reentry velocity than the configuration shown as (5). That is to say, reentry mode and severity are coupled with configuration. It is recommended that further analysis of the range of reentry configurations and modes be conducted by superimposing, on the computed $V-\gamma$ plot, lines of constant time (from TE 364-4 burnout) corresponding to TE 364-4/spacecraft separation and RTG boom deployment. In this manner, the initial reentry conditions on the $V-\gamma$ plot, and the corresponding configurations, can be related, thus allowing concentration on the reentries of primary interest.

Table 3-2. Summary of Potential Reentry Configurations

<u>Configuration</u>	<u>Orbital Decay</u>	<u>Reentry Mode</u>		<u>Prompt</u>
		<u>Graze</u>	<u>Skip (1st Pass)</u>	
RTGs	1			
Spacecraft (booms deployed)	2	5	8	11
Spacecraft (booms undeployed)	3	6	9	12
TE 364-4 (empty)/ spacecraft (booms undeployed)		7	10	13
Centaur (empty)/ TE 364-4 (full)/ spacecraft (booms undeployed)	4			

4. SPACECRAFT/RTG BREAKUP ANALYSIS

Of the potential reentry configurations discussed in Section 3.0, two were selected to be analyzed in this study to determine the conditions at which the RTGs or nuclear heat sources become separated from the spacecraft during reentry. The first configuration consisted of the Centaur (propellants depleted)/TE 364-4 (propellant intact)/spacecraft in a random orbital decay mode, which may be caused by a flight programmer failure immediately after a successful Centaur thrust phase. The second configuration consisted of the TE 364-4 (propellant depleted)/spacecraft in a superorbital reentry resulting from pitch attitude misorientation at TE 364-4 ignition. These configurations are shown in Figure 4-1 with their major dimensions. For both configurations, the RTGs were assumed to be undeployed, but the likelihood of deployment during reentry was assessed. The trimmed attitudes of both configurations during reentry was estimated, and both trimmed and tumbling reentry modes were investigated. The general procedure followed in all cases was to:

- o determine the aerodynamic properties and establish the initial reentry conditions
- o compute the reentry trajectory, aerodynamic heating, and aerodynamic pressure histories
- o determine which components were critical and the heating rate factors to be applied to these components
- o calculate the temperature histories of critical components
- o calculate the loads applied to the critical components, their allowable loads, and determine the times of failures

The details of the analysis are discussed in the following sections.

4.1 RANDOM ORBITAL DECAY

The aerodynamic drag coefficients and initial reentry conditions used for the Centaur/TE 364-4/spacecraft configuration in a random orbital decay reentry are shown in Table 4-1. The configuration, dimensions, and weights of the Centaur, interstage structure, and TE 364-4 were supplied by General Dynamics/Convair (GD/C). An aerodynamic study was also performed by GD/C in which a statically stable trim point and the continuum drag

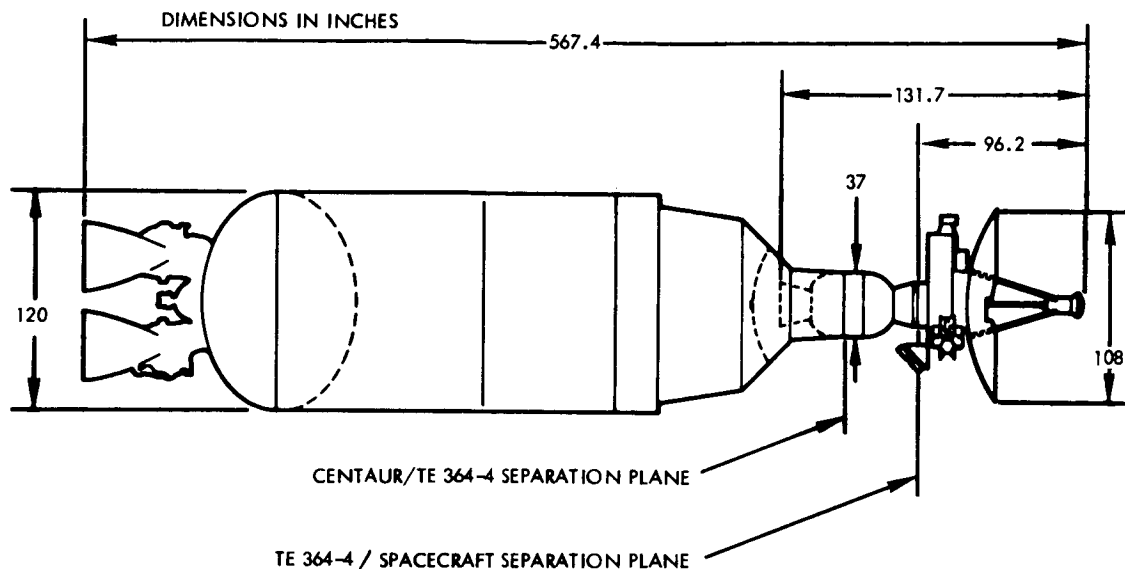
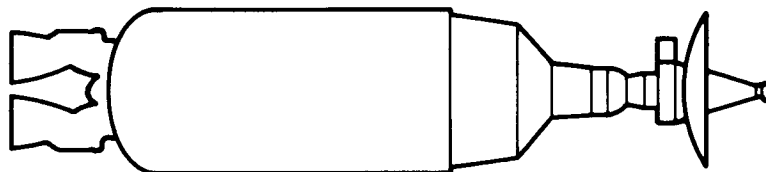


Figure 4-1. Dimensions of Configurations

Table 4-1. Random Orbital Decay Assumptions

Configuration



Centaur (Empty)/TE 364-4 (Full)/Spacecraft

Aerodynamic Drag Coefficients

Tumbling	3.75
Trimmed ($\alpha=50^\circ$)	3.10
Reference Area	78.5 Ft ²

Initial Conditions

Altitude	400,000 Ft.
Latitude	0 ⁰
Longitude	0 ⁰
Inertial Velocity	25705 Ft./Sec.
Inertial Flight Path Angle	0.08 ⁰ (Down)
Inertial Azimuth	121.4 ⁰
Weight	7727 Lb.

coefficients corresponding to trimmed and tumbling reentry were determined by Newtonian theory. These drag coefficients were reviewed and verified by TRW.

The initial reentry conditions shown in Table 4-1 were used for both tumbling and trimmed cases. The initial reentry altitude of 400,000 ft. was at first selected based on the assumption that the atmosphere above this altitude would have negligible effect on the reentry results. As will be discussed later in this report, this assumption was later found to be invalid, and reentry was then assumed to start at 450,000 ft. However, the trajectory passes through 400,000 ft. with the conditions shown in Table 4-1. Since, in a random orbital decay situation the exact latitude and longitude of reentry cannot be predicted with accuracy because of uncertainties in ballistic coefficient, solar variations and their effects on atmospheric density, etc., the latitude and longitude in this case were both arbitrarily selected as zero degrees. The inertial velocity was calculated from Reference 4-1 and assumed the earth to be a homogeneous sphere. The flight path angle was computed from the relationship presented in Reference 4-2 for decaying spacecraft, which yielded flight path angles of .05 degree to 0.10 degree below the local horizontal, corresponding to the use of continuum and free molecule drag coefficients, respectively. A previously computed orbital decay trajectory for an Atlas Agena vehicle, which was determined by TRW during a hazard study, gave a value of 0.08 degree. The value of 0.08 degree flight path angle was used in this breakup study since this value was in agreement with the range of calculated values. The value of inertial azimuth was determined from the average orbital inclination possible over the spectrum of nominal trajectories presented in Reference 4-3. The weight of the configuration was supplied by GD/C.

The trajectory, aerodynamic pressure and aerodynamic heating histories were computed using the Position and Time History (PATH) program with the point mass option. This program computes the position and state vector of a rigid vehicle by numerically integrating the differential equations of motion from a prescribed initial position. The program uses an ellipsoidal earth model in conjunction with a 1962 standard atmosphere model. Altitude as a function of time is shown in Figure 4-2 and Figure

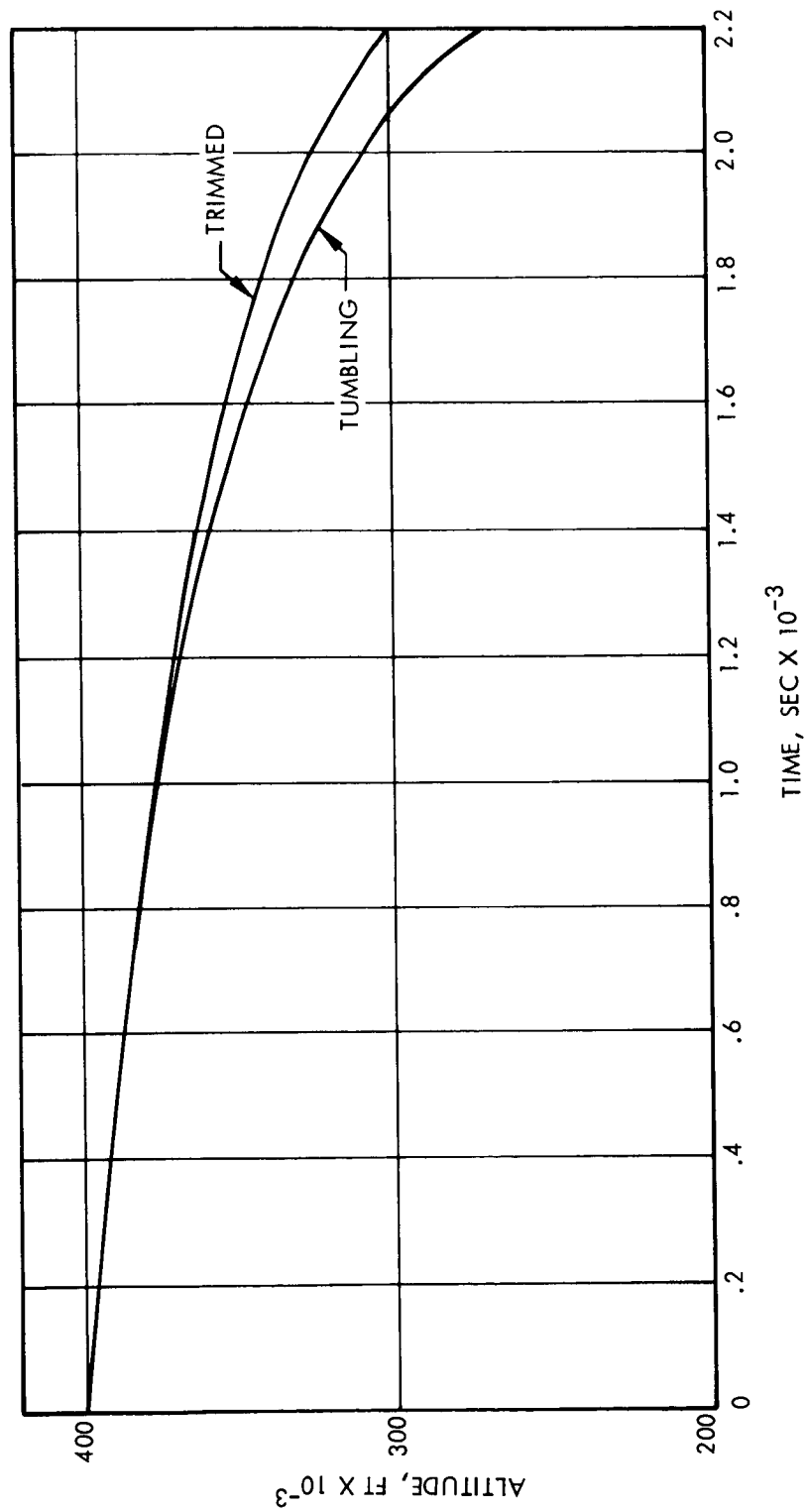


Figure 4-2. Orbital Decay Trajectory History

4-3 shows the dynamic pressure history.

The modes of heat transfer analyzed in determining the reentry heating rates were convection, re-radiation, gas-cap radiation, and conduction. The convective heating rate to a particular body is a function of the trajectory and the geometry of the body (i.e. size, shape, and shading). Trajectory and geometry effects were separated by considering the convective heating rate to the stagnation point of a standard body and then applying a geometry factor, K_s , to this rate.

For free molecule flow, the standard body is a flat plate normal to the flow with the back surface insulated. The heating rate per unit area is*

$$\dot{q}_s = \frac{\mu}{Z} \rho_\infty V_a^3 \quad (4-1)$$

For continuum flow, the standard body is a one-foot radius sphere, and, from Reference 4-4, the stagnation point heating rate is

$$\dot{q}_s = (0.84 \times 10^{-8}) \rho_\infty^{0.5} V_a^{3.08} \left(1 - \frac{H_{ws}}{H_e} \right) \quad (4-2)$$

The convective heating rates defined by Equations 4-1 and 4-2 are shown in Figure 4-4. The transition from free molecule heating to continuum heating occurs when the heating rates are equal, and this point depends on the geometry and size of the body. For the random orbital decay case, transition was taken to occur when the continuum heating rate on the stagnation line of a ten-foot diameter cylinder (i.e. Centaur configuration) equalled the free molecule heating rate.

Radiation heat transfer was considered in determining the temperature histories of the critical components. The rate of change of altitude was sufficiently slow in the orbital decay case that significant cooling occurs due to reradiation. The reradiation rate is

$$\dot{q}_R = K_R \epsilon \sigma T^4 \quad (4-3)$$

Radiation to a surface from the hot gas in the stagnation region (i.e. gas cap radiation) was initially considered but was found to be negligibly small and was therefore not included.

*See Appendix A, Nomenclature

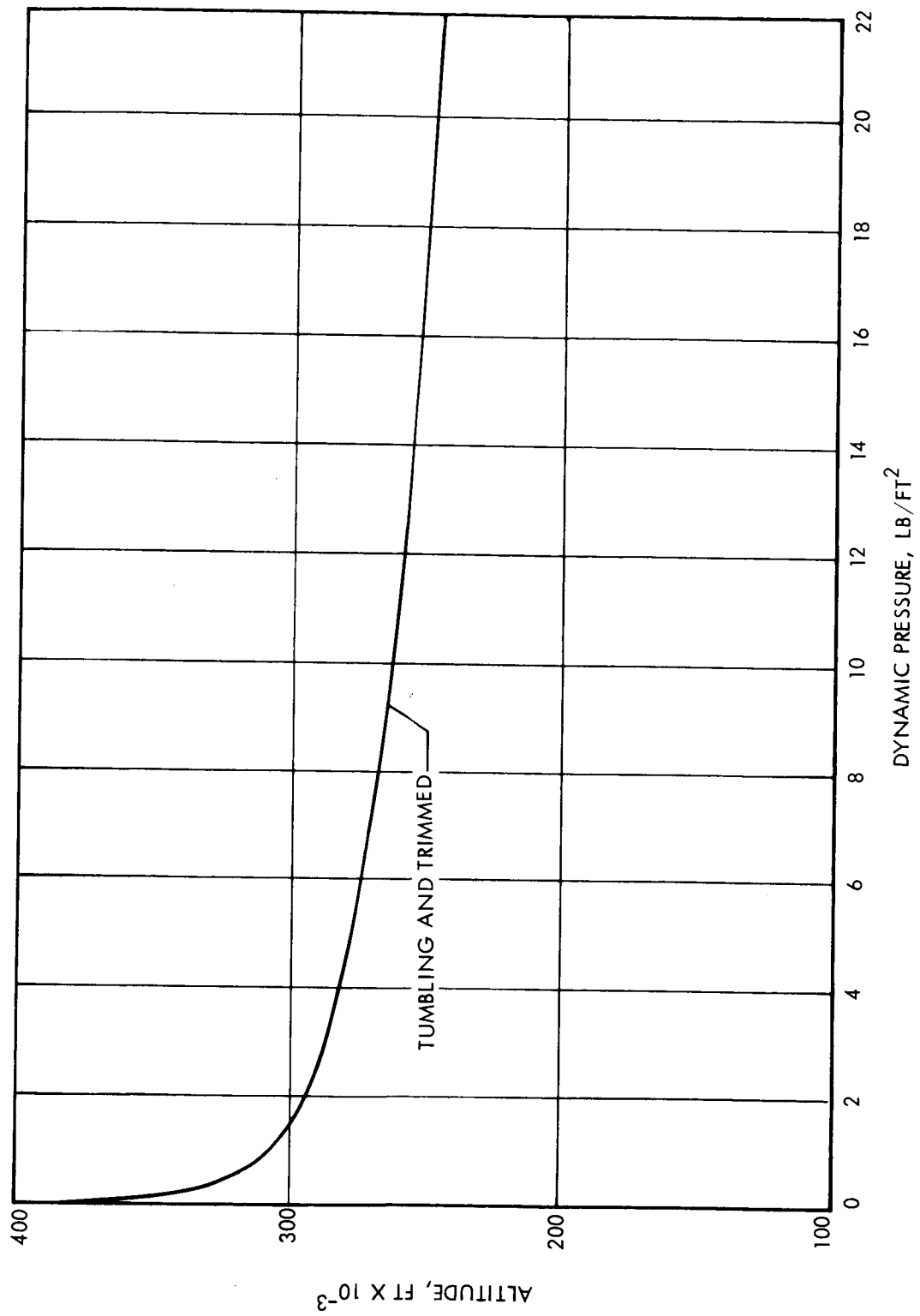


Figure 4-3. Orbital Decay Dynamic Pressure History

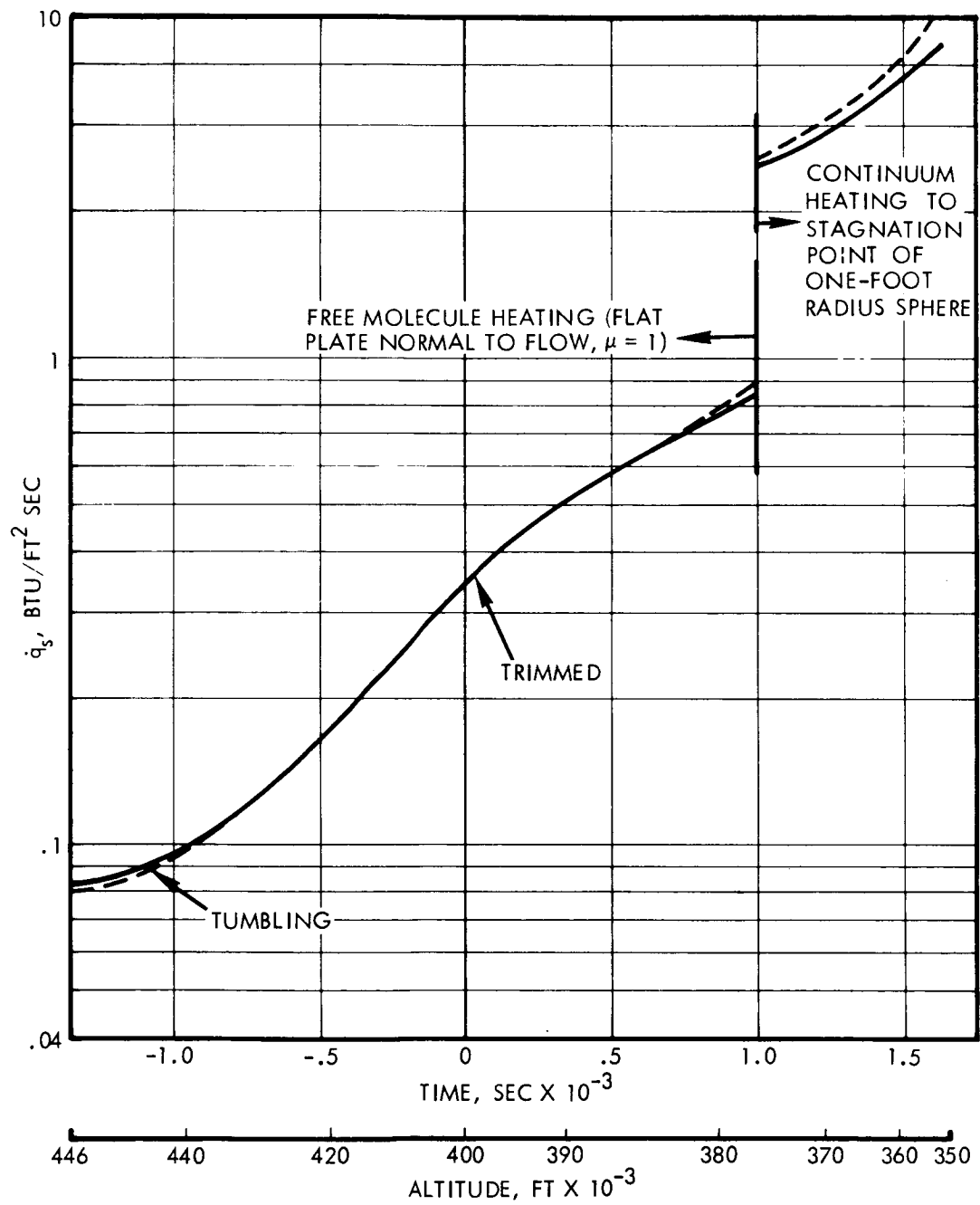


Figure 4-4. Orbital Decay Stagnation Heating Rate History

As shown in Table 4-1, initial reentry conditions were defined at 400,000 feet altitude. However, initial calculations of breakup altitude indicated that the contribution from heating above 400,000 ft. was significant. Therefore, the trajectories were "backed-up" by reversing the sign of the reentry angle and the drag. A local altitude maximum, before the final reentry, was found near 450,000 ft. altitude, and the heating calculations were therefore started at this altitude.

At this point in the analysis it was necessary to determine the types of events that could affect RTG separation conditions in order to identify the critical components. The following events were identified:

- 1) Separation of Centaur from TE 364-4
- 2) Auto-ignition of TE 364-4 propellant
- 3) Separation of TE 364-4 from spacecraft
- 4) Spacecraft reflector failure
- 5) Separation of RTG from spacecraft, or nuclear heat sources from RTG

Although determining the altitude at which event 5 occurred was the primary goal of the study, events 1 through 4 could affect the conditions of RTG or nuclear heat source release from the spacecraft.

For each event, with the exception of event 2, a critical component was identified which had the lowest heat capacity per unit of exposed surface area. For a thin skin (i.e. a component whose thickness is small compared with a typical lateral dimension) the total heat capacity per unit area is

$$\rho h C_p (T_f - T_i)$$

From current Pioneer spacecraft drawings and from descriptions of the launch vehicle hardware in Reference 4-5, the following critical components were identified as causing the events discussed above:

- Event 1) Stub Adaptor (part of Centaur/TE 364-4 adaptor)
- 3) TE 364-4/Spacecraft Interstage Adaptor
 - 4) Reflector
 - 5) RTG Support Truss

The properties of the Stub Adaptor, Reflector, and Support Truss are listed in Table 4-2. The properties of the TE 364-4/Spacecraft Inter-stage Adaptor are not shown because subsequent analyses indicated that this component is sufficiently thick (.070 in. minimum) that it would not fail before RTG separation. Note that failure temperature, T_f , is not known a priori. However, T_f is usually close to the melting temperature. Properties of the TE 364-4 motor case and propellant are also listed in Table 4-2. Since the "thin skin" approximation is not valid in predicting event 2, thermal conductivities of the motor case and propellant were required and are also shown in Table 4-2.

The heating rates shown in Figure 4-4 were multiplied by geometry factors, K_s , to account for the shape, size, and shading of individual components. The geometry factors are given in Table 4-3 for the case of random orbital decay. Table 4-3 also gives the radiation shape factors, K_p , and emissivities, ϵ , used for the orbital decay cases. The geometry factors for continuum flow are based on the data of References 4-4 and 4-6 and the spacecraft structural configuration. The geometry factors for free molecule flow are ratios of the average exposed area projected forward, along the flight path, to the total area. For flat plate elements such as the Reflector dish and RTG fins, the total area was taken to be the area of one side. The exposure differs, in general, for the different legs of the RTG Support Truss and for the two RTGs in a pair. The geometry factors given are for the element with the greatest exposure.

Failure of the Reflector or Stub Adaptor will result in both changes in the geometry factors, K_s , of certain components and in the ballistic coefficient, β , of the configuration. As shown in Table 4-3, changes in K_s were considered in the calculations. However, changes in β were not included in the calculations because the integrated heating rate is relatively insensitive to these changes. This was verified for the trimmed, prompt reentry case discussed in Section 4.2, which is the case where the greatest trajectory change would be expected. A new β was estimated after melting of the Reflector, and a new trajectory was calculated from this point. The resulting increase in \dot{q}_s , due to an increased velocity, was almost exactly compensated by the increase in

Table 4-2. Critical Component Properties

Component	Material	Material Thickness (in.)	Density lbm/ft ³	Specific Heat BTU/lbm °R	Melting Temperature °F	Conductivity BTU/ft ² -sec °F
Stub Adaptor	2219-T81 Alum.	.032	178	.22	1100	-
Reflector	Alum.	.633	3.86*	.22	1060	-
RTG Support Truss	2024-T351 Alum.	.052**	173	.22	1060	-
Third Stage Motor Case (Front Hemisphere)	Ti 6Al 4V	.052	276	.135	3000	.00117
Third Stage Propellant***		$11 \leq h \leq 16.4$	109	.24	-	.000464

*Average: consists of 2-4 mil face sheets ($\rho = 173 \text{ lbm/ft}^3$), 5/8" aluminum honeycomb ($\rho = 1.6 \text{ lbm/ft}^3$).

**Average: truss legs are I-beams with 3/4 x .055 flanges and 3/4 x .045 web.

***Minimum auto-ignition temperature = 570°F.

Table 4-3. Geometry Factors - Orbital Decay

MOTION/FLOW REGIME	COMPONENT											
	Stub Adaptor			3rd Stage Motor			Reflector			RTG Support		
	K _R	ε	K _S	K _R	ε	K _S	K _R	ε	K _S	K _R	ε	K _S
<u>TUMBLING</u>												
Free Molecule Flow	1	.1	.20	-	-	-	1.5*	.1	.20	2/3	.1	.167
Continuum Flow	1	.1	.07	-	-	-	1.5*	.1	.085	2/3	.1	.064
<u>TRIMMED ($\alpha = 50^\circ$)</u>												
Free Molecule Flow Before Refl. Failure	1	.1	.244	1	.2	.41	1.5	.1	.643	2/3	.1	.092
Free Molecule Flow After Refl. Failure	1	.1	.244	1	.2	.41	-	-	-	.9	.1	.214
Continuum Flow Bef. Stub Adaptor Failure	1	.1	.12	1	.2	.136	-	-	-	**	**	**
Continuum Flow Aft. Stub Adaptor Failure	-	-	-	1	.2	.086	-	-	-	.9	.1	.064

*K_R > 1 because reference area is area of one side.

**Stub adaptor failure occurs soon after transition to continuum flow and was assumed to occur at transition for this calculation.

***Tumbling motion assumed.

rate of change of altitude; resulting in negligible change in the integrated heating rate between the altitudes of Reflector failure and predicted RTG/Spacecraft separation.

Temperature histories of the Reflector and RTG Support Truss for the tumbling reentry mode are shown in Figure 4-5. The Stub Adaptor temperature history is not shown because its failure will not cause a change in the geometry factors. The temperature histories were obtained by integrating the equation,

$$\rho h C_p \frac{dT}{dt} = K_s \dot{q}_s - K_F \epsilon \sigma T^4 \quad (4-4)$$

where the initial temperatures were chosen so that dT/dt vanished at the initial altitude; that is to say, so that local equilibrium prevailed between convective heating and reradiation. As shown in Figure 4-5, melting of the reflector and RTG Support Truss occurs at approximately 355,000 ft. The dynamic pressure at this altitude was referenced to determine if aerodynamic loading would cause Reflector or Support Truss failure at an altitude above that predicted for melting. As shown in Figure 4-3, the dynamic pressure at 355,000 ft. is approximately 0.1 lb/ft^2 , which was considered to have negligible effect. Therefore, 355,000 ft. was predicted to be the breakup altitude for the tumbling reentry mode.

Temperature histories of the Reflector, Stub Adaptor, and RTG Support Truss for the trimmed reentry mode are shown in Figure 4-6. These temperatures were obtained as for the tumbling reentry mode except that the initial temperature of the RTG Support Truss represents an equilibrium between conductive heating (from the RTGs) and reradiation. The convective heating rate was assumed to be negligible compared to the heat conducted into the Support Truss from the RTGs because of the shading afforded by the Reflector. The effect of conduction on the temperature histories of the RTG Support Truss was included by fairing the solution given by Equation 4-4 into the line $T=T_i=325^\circ\text{F}$. The Stub Adaptor temperature shown in Figure 4-6 was considered in the case of trimmed reentry because loss of the Centaur stage was assumed to result in a tumbling motion of the resulting TE 364-4/Spacecraft configuration and, therefore, a change in the geometry factors. The Reflector temperature

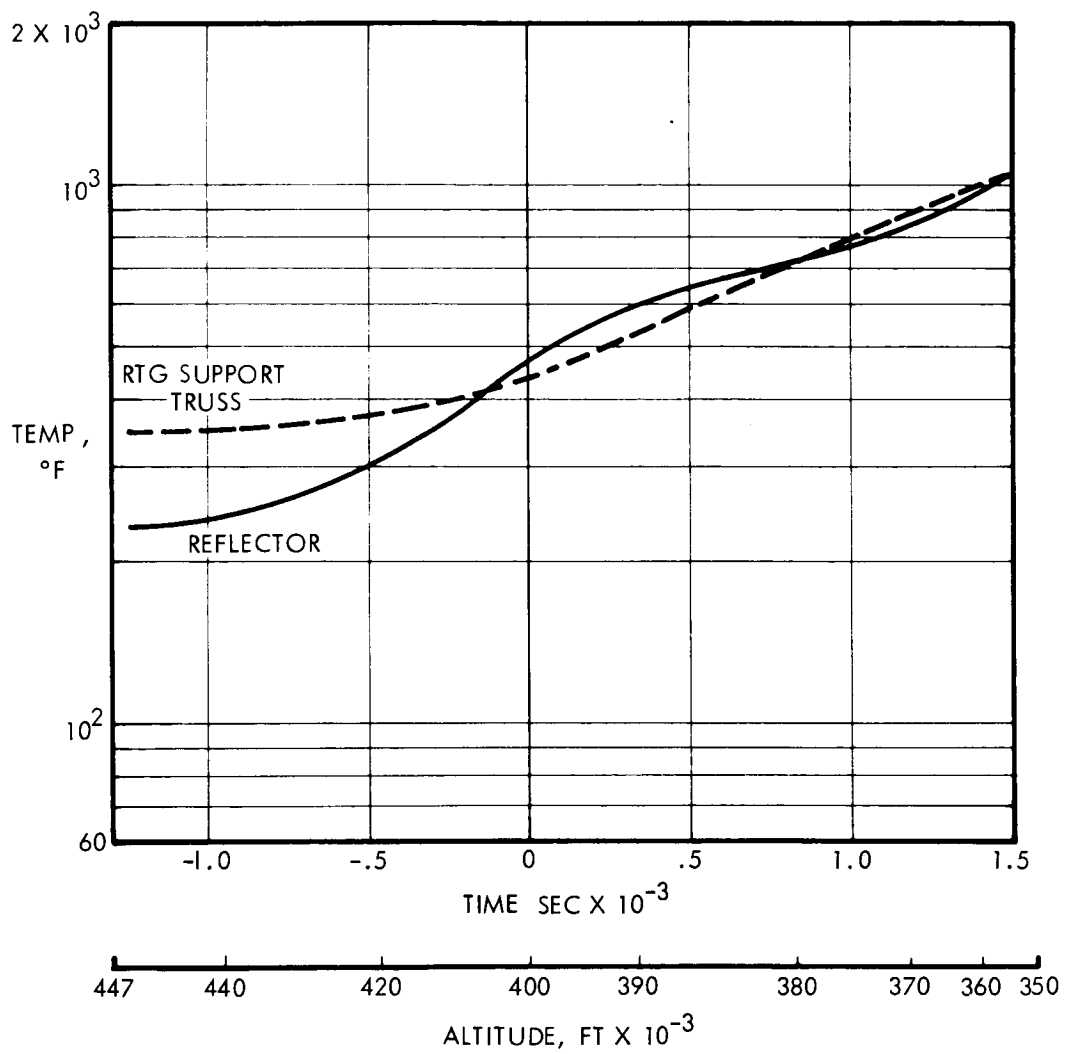


Figure 4-5. Component Temperature Histories:
Orbital Decay, Tumbling

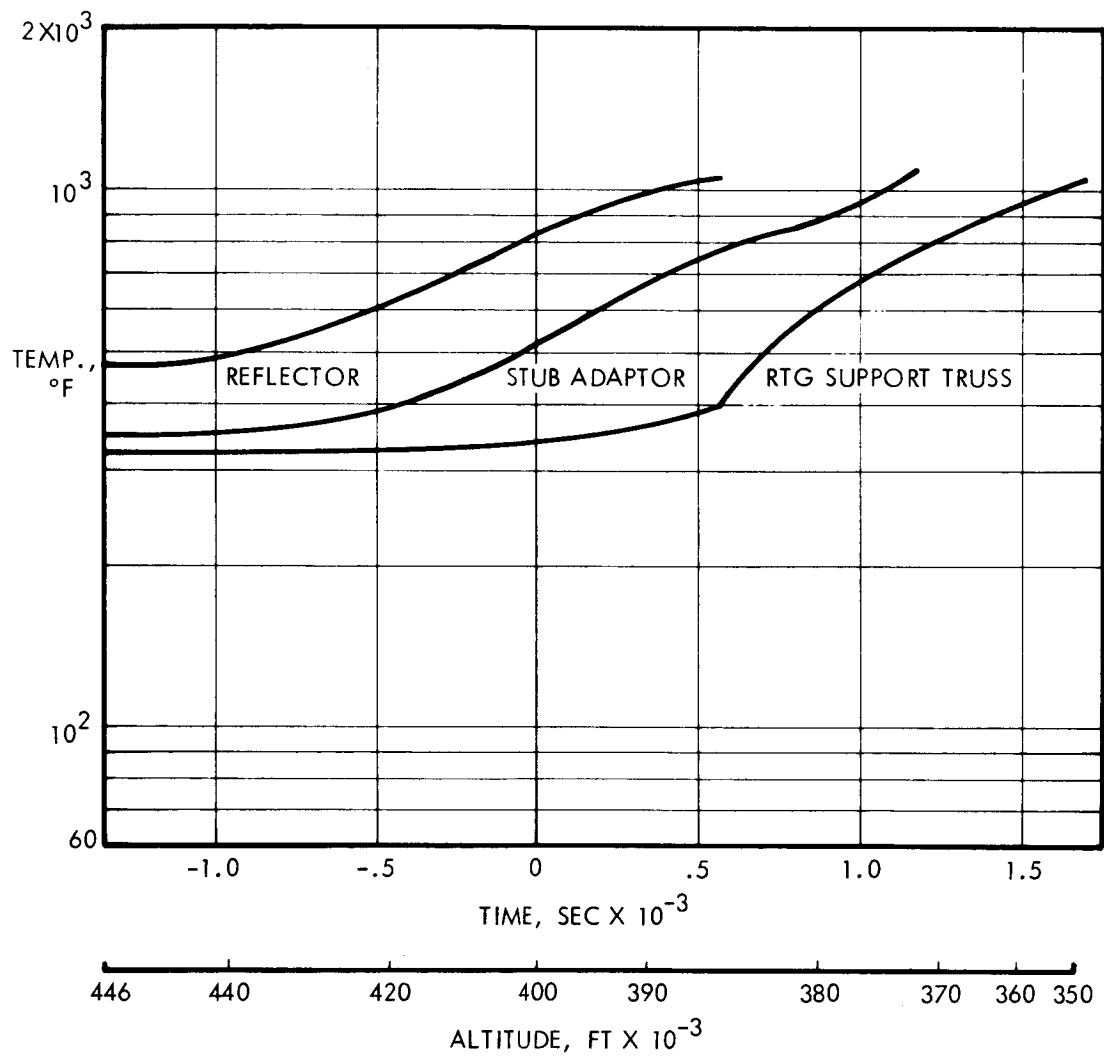


Figure 4-6. Component Temperature Histories:
Orbital Decay, Trimmed

is similarly included in Figure 4-6 because it shrouds the RTG and RTG Support Truss from heating, and its loss subsequently increases the heating to these components. As can be seen in Figure 4-6, the Reflector melts at approximately 387,000 ft., causing a marked increase in the rate of change of RTG Support Truss temperature. Approximately 700 seconds later, at an altitude of about 372,000 ft., the Stub Adaptor fails, causing separation of the Centaur stage, tumbling of the TE 364-4/spacecraft configuration, and reduced heating to the RTG and Support Truss. Finally, at an altitude of approximately 347,000 feet, melting of the Support Truss occurs, thus releasing the RTGs. As was the case for the tumbling reentry mode, it was assumed for the trimmed mode that the negligible aerodynamic pressure at this altitude would not cause structural failure significantly above the altitude at which Support Truss melting was predicted.

Figure 4-7 presents the temperature history of the RTGs housing up to separation from the spacecraft for both tumbling and trimmed reentries. The initial temperature was chosen to be 355°F, corresponding to equilibrium between conduction from the heat source and reradiation. In the transient analysis reradiation and the heat generated by the nuclear heat sources were included. For this case, Equation 4-4 becomes,

$$\frac{C_p W}{A_{RTG}} \frac{dT}{dt} = K_S \dot{q}_S + \dot{q}_D - K_R \epsilon \sigma T^4 \quad (4-5)$$

where $\dot{q}_D = 610 \text{ watts}/A_{RTG}$, and $C_p W/A_{RTG}$ is an effective heat capacity per unit area. The effective heat capacity was taken to be the sum of the heat capacities of only the delta frame, housing assembly, and heat sink assembly because thermal contact between the container and the remaining RTG components is relatively poor. The heat capacities of the pertinent RTG components and the delta frame between the RTG pairs are given in Table 4-4. As can be seen in Figure 4-7, RTG temperature at separation is approximately 490°F for the tumbling reentry mode and 500°F for the trimmed mode, which are both well below the RTG housing melt temperature.

When the RTG Support Trusses fail, thus releasing the intact RTGs in pairs, the damper cable normally used in deploying the RTGs, and the electrical cable from the RTGs to the spacecraft, will be attached. However it can be assumed that the RTGs, because of their greater ballistic

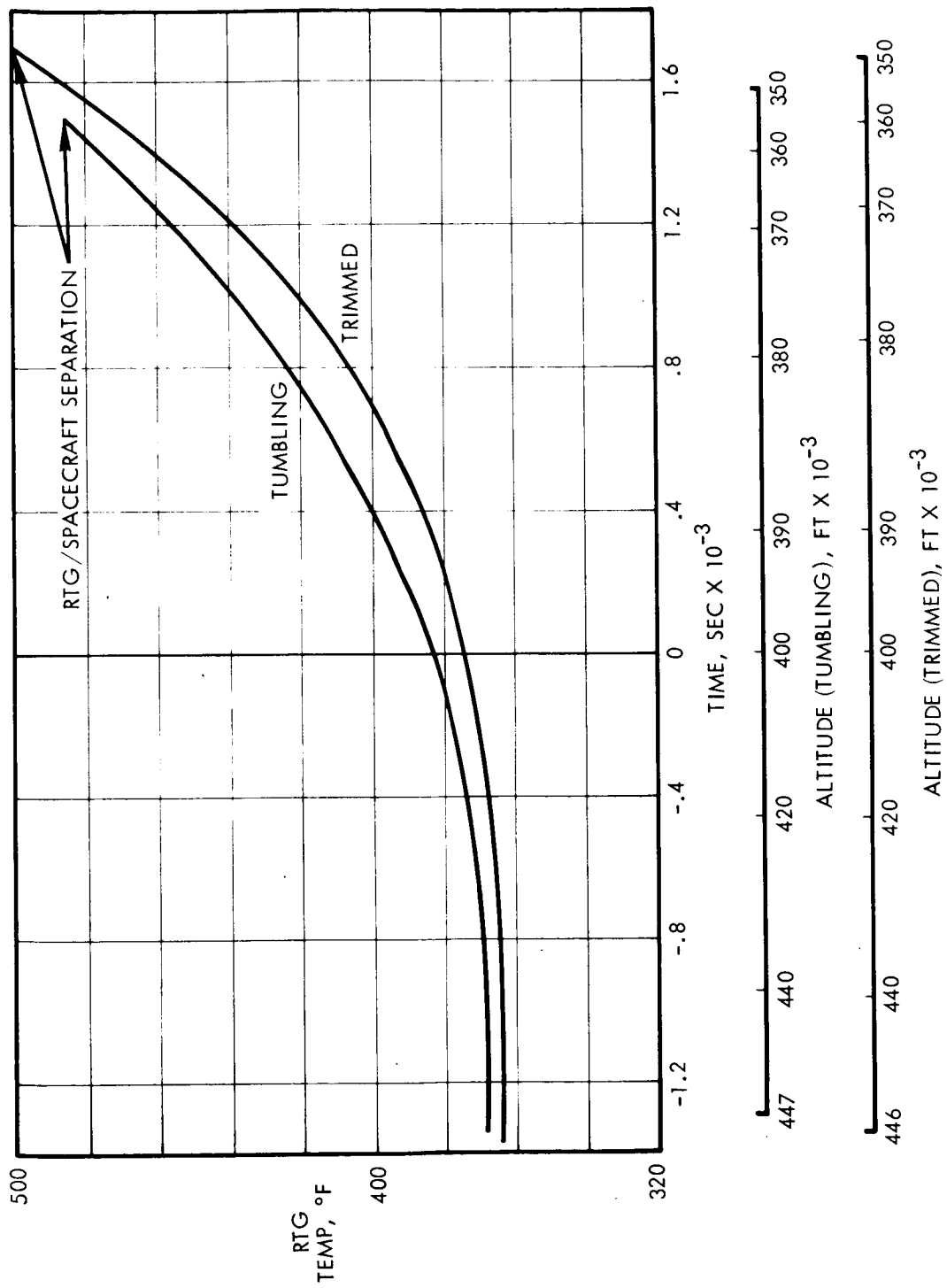


Figure 4-7. RTG Housing Temperature History During Orbital Decay

Table 4-4. Heat Capacities of Delta Frame and RTG Components

Component	Weight lb	Major Material	Specific Heat BTU/lb ^o R	WC _P BTU/ ^o R
Delta Frame	1.3	Alum.	.22	0.29
RTG Components				
Housing Assembly	9.944	MgTh	.25	2.49
Heat Sink Assembly	3.822	Al	.23	0.88

coefficients, will immediately accelerate away from the spacecraft, out to a distance of approximately 6 ft. (i.e., the deployed length of the cables). In this event, the RTGs and cables will probably be outside the bow shock created by the TE 364-4/spacecraft, and will immediately experience stagnation heating. It is anticipated that in this environment, both the RTG damper cable (1/16 in. dia., phosphor bronze) and the electrical cable (5 mils thick x 3 in. wide, Al. alloy ribbon with insulation) will fail rapidly.

A thermal analysis of the TE 364-4 motor during reentry was made to determine whether propellant auto-ignition could occur prior to RTG separation. From Reference 4-7 and liaison with GD/C, it was determined that auto-ignition could not occur below 300^oC (572^oF), and above this temperature, auto-ignition was a temperature/time phenomenon. The trimmed reentry mode was conservatively selected for investigation because this trajectory results in the highest heating applied to the motor casing. Figure 4-8 presents the temperature history at the motor case/propellant interface in an annular region of the forward hemisphere. This temperature history was computed using TRW's Conduction-Ablation-Reaction-Erosion computer program, which solves the Fourier heat conduction problem in one dimension using finite differences and can include surface and indepth chemical reaction or phase change. The initial temperature was assumed to be 80^oF, and peak temperature at RTG separation was computed to be 415^oF. Based on this result, auto-ignition of the TE 364-4 during random orbital decay is not predicted to occur prior to separation of the RTGs.

The RTG release conditions are summarized in Table 4-5.

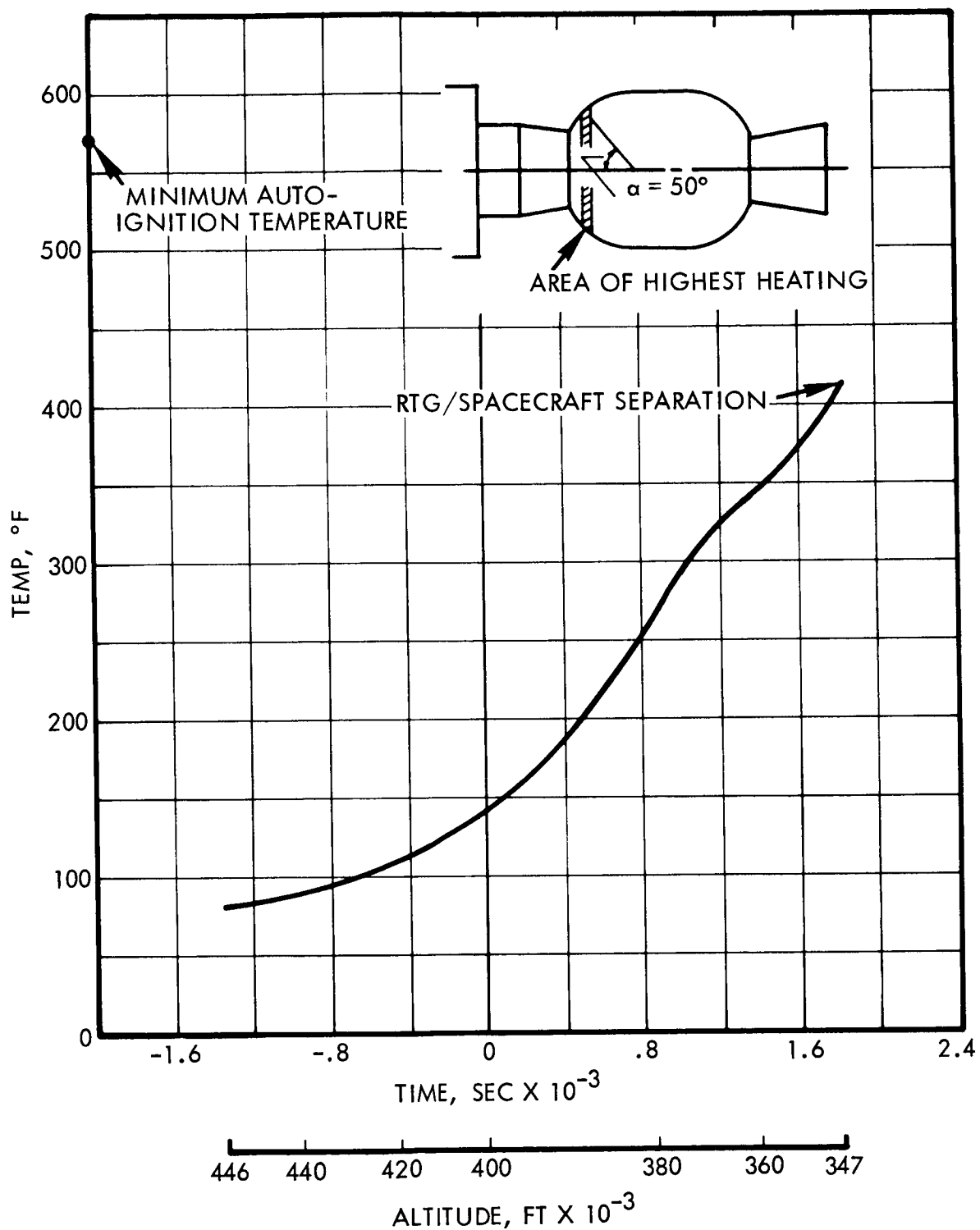


Figure 4-8. Temperature History of TE 364-4 Propellant at Case/Propellant Interface in the Area of Highest Heating: Orbital Decay-Trimmed

Table 4-5. Random Orbital Decay

<u>Conditions at RTG Release</u>	<u>Tumbling</u>	<u>Trimmed</u>
Altitude	355,000 Ft.	347,000 Ft.
Latitude	30.508 ⁰ S	27.375 ⁰ S
Longitude	99.767 ⁰ E	115.134 ⁰ E
Inertial Velocity	25,720 Ft./Sec.	25,722 Ft./Sec.
Inertial Flight Path Angle	0.110 ⁰ (Down)	.098 ⁰ (Down)
Inertial Azimuth	81.655 ⁰	73.773 ⁰
RTG Temperature	490 ⁰ F	500 ⁰ F

4.2 PROMPT REENTRY

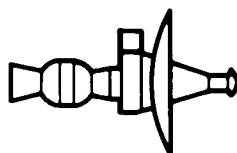
The procedure that was followed in predicting RTG release conditions from the TE 364-4/spacecraft configuration during a superorbital, prompt reentry was generally identical to the procedure discussed in Section 4.1. However, whereas the prompt reentry case did not require analysis of the potential auto-ignition of the TE 364-4 during reentry, because the propellant is utilized prior to reentry, the prompt reentry case did require detailed investigation of the initial reentry conditions and of the structural loading during reentry.

The statically stable trim point and the continuum drag coefficients corresponding to trimmed and tumbling reentry were determined by GD/C using Newtonian theory. These drag coefficients were reviewed and verified by TRW, and are presented in Table 4-6. The approach used in determining the initial reentry conditions shown in Table 4-6 is discussed in the following paragraphs.

For this study, it was required to select a high reentry velocity, shallow flight path angle condition which would cause the RTGs to remain within the atmosphere after release from the spacecraft. Of the spectrum of nominal launch trajectories, five representative nominal trajectories which bound the spectrum are currently being investigated by GD/C (Reference

Table 4-6. Prompt Reentry Assumptions

Configuration



TE 364-4 (Empty)/Spacecraft

Aerodynamic Drag Coefficients

Tumbling	1.11
Trimmed ($\alpha=0^\circ$)	1.59
Reference Area	78.5 Ft ²

Initial Conditions (resulting from 50° pitch down misorientation)

Altitude	400,000 Ft.
Latitude	17.04°N
Longitude	323.04°E
Inertial Velocity	42,740 Ft./Sec.
Inertial Flight Path Angle	8.33° (Down)
Inertial Azimuth	113.48°
Weight	763 Lb.
Time From Liftoff	862 Sec.

4-8). The initial reentry conditions resulting from pitch and yaw attitude misorientations of the TE 364-4 during each of the five nominal trajectories are also being investigated. The highest potential reentry velocities result from aborts during launches at the beginning (i.e. relative launch time of 14 hours, 0 minutes) of the one-hour launch period being investigated. Figure 4-9 represents the flight path angle and velocity at 400,000 ft. resulting from pitch down attitude misorientation of the TE 364-4 during these early launches, based on preliminary data supplied by GD/C. Aborts during the other three nominal trajectories, launched later in the one-hour period, result in lower reentry velocities.

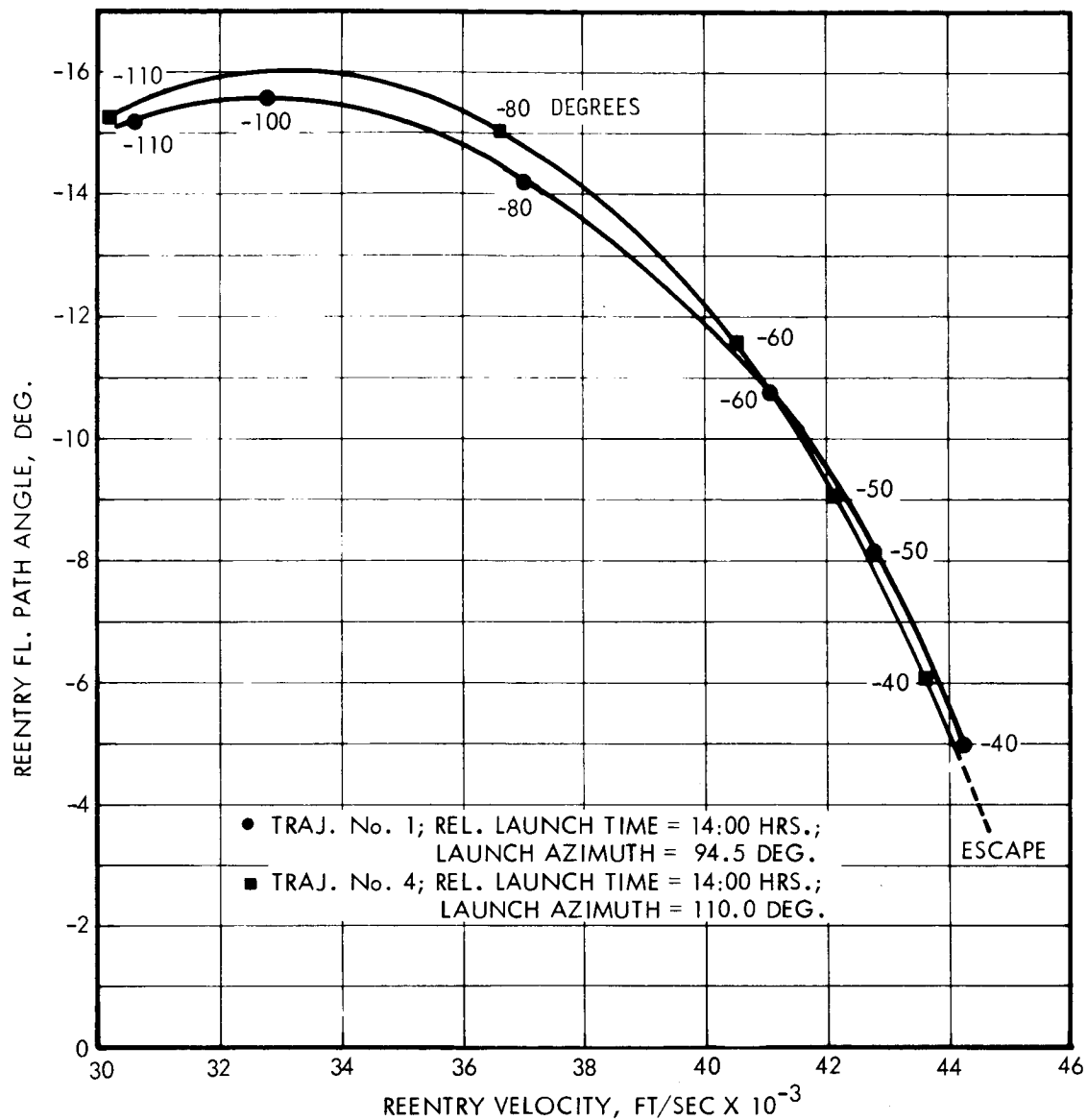


Figure 4-9. Pioneer F Reentry Conditions (at 400 kft)
Due to TE 364-4 Pitch Down Misorientations
at Ignition

From Figure 4-9, Trajectory number 4, a pitch down misorientation of 40 degrees was selected to determine a prompt return trajectory. The altitude history of this trajectory was computed and is shown in Figure 4-10. Separation altitudes of 300,000 ft., 250,000 ft., and 200,000 ft. were arbitrarily selected and RTG trajectories after separation were computed by assuming a ballistic coefficient, β , of 40 lb/ft². As can be seen in

Figure 4-10, if separation occurred at 300,000 ft. or 250,000 ft. the RTGs were found to leave the atmosphere, passing upward through the altitude of 400,000 ft. with velocities of 30,000 to 32,000 ft/sec. The RTGs would then have undergone multiple-skip reentry. A preliminary breakup analysis was conducted which indicated that breakup would actually occur at an altitude of approximately 263,000 ft. Since according to Figure 4-10 breakup at this altitude would cause the RTG to skip out, the 40 degree pitch down case was not investigated further.

The next selection of initial reentry conditions corresponded to a pitch down misorientation of 50 degrees, Trajectory #1. Release altitudes of 300,000 ft. and 263,000 ft. were assumed, and the resulting RTG trajectories were computed. The results are shown in Figure 4-11, where it can be seen that breakup at these altitudes would subsequently result in a prompt reentry of the RTGs. The 50° misorientation case was therefore selected for detailed analysis. The initial reentry conditions corresponding to this misorientation are shown in Table 4-6. The spacecraft dynamic pressure history corresponding to the trajectory of Figure 4-11 is shown in Figure 4-12.

It was apparent from the trajectory analysis discussed above that a narrow range of attitude misorientations lay between 40 degrees and 50 degrees that would result in grazing reentries, in which altitude could remain constant for a period of time during reentry, as shown in Figure 4-13, or might even increase slightly after this altitude plateau before terminal reentry. An accurate determination of the bounds of attitude misorientations resulting in these grazing reentries was not included in this study and the 50° pitch down case, for which reentry conditions were available, was studied.

The convective heating rate was obtained using Equations 4-1 and 4-2 and is shown in Figure 4-14. The heating rates for tumbling and trimmed reentries are essentially equal. As was the case for random orbital decay, discussed in Section 4-1, heating due to gas cap radiation was found to be negligible. Reradiation was also investigated and was found to be negligible in the case of prompt reentry.

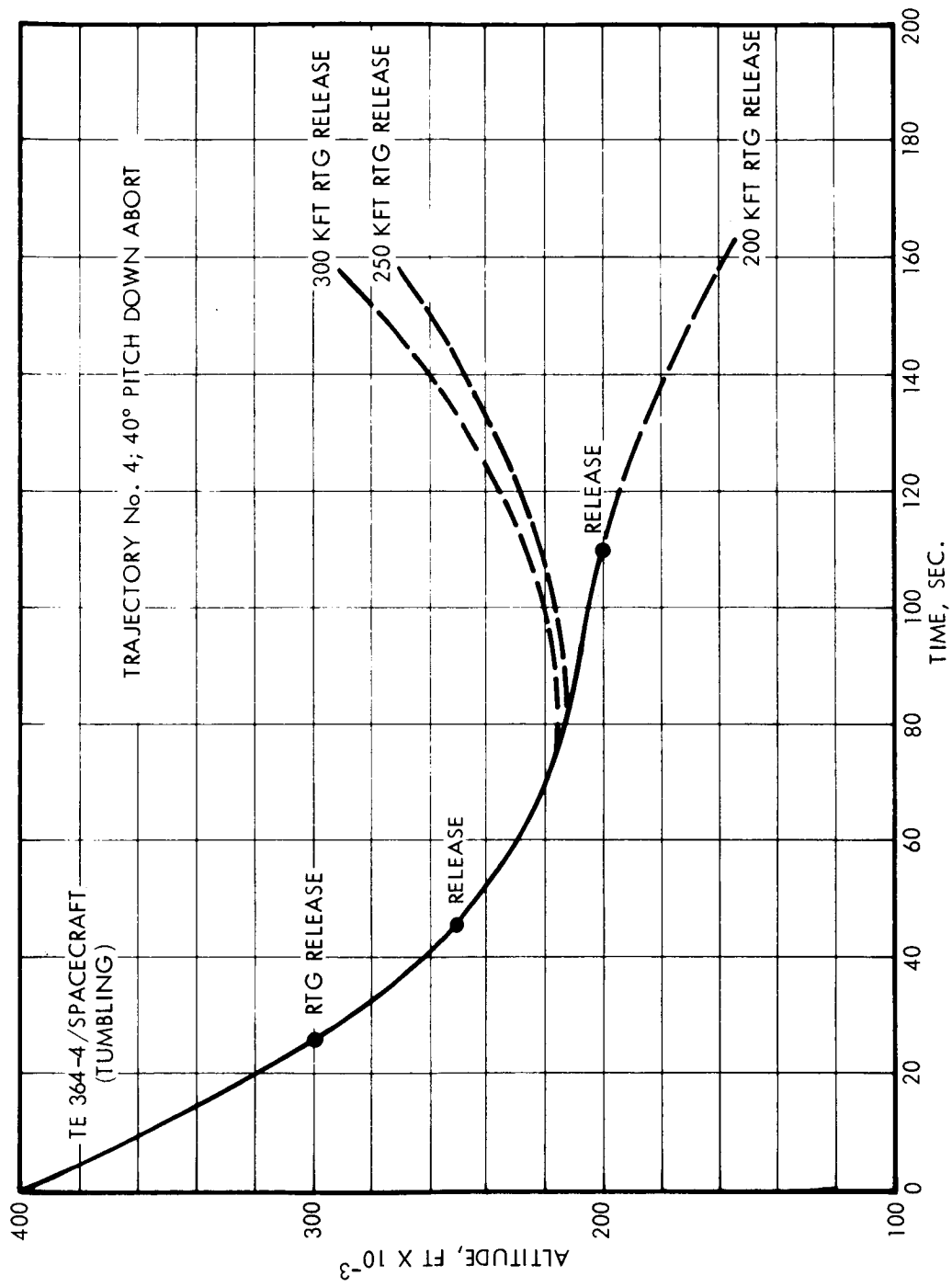


Figure 4-10. Prompt Reentry Trajectory History

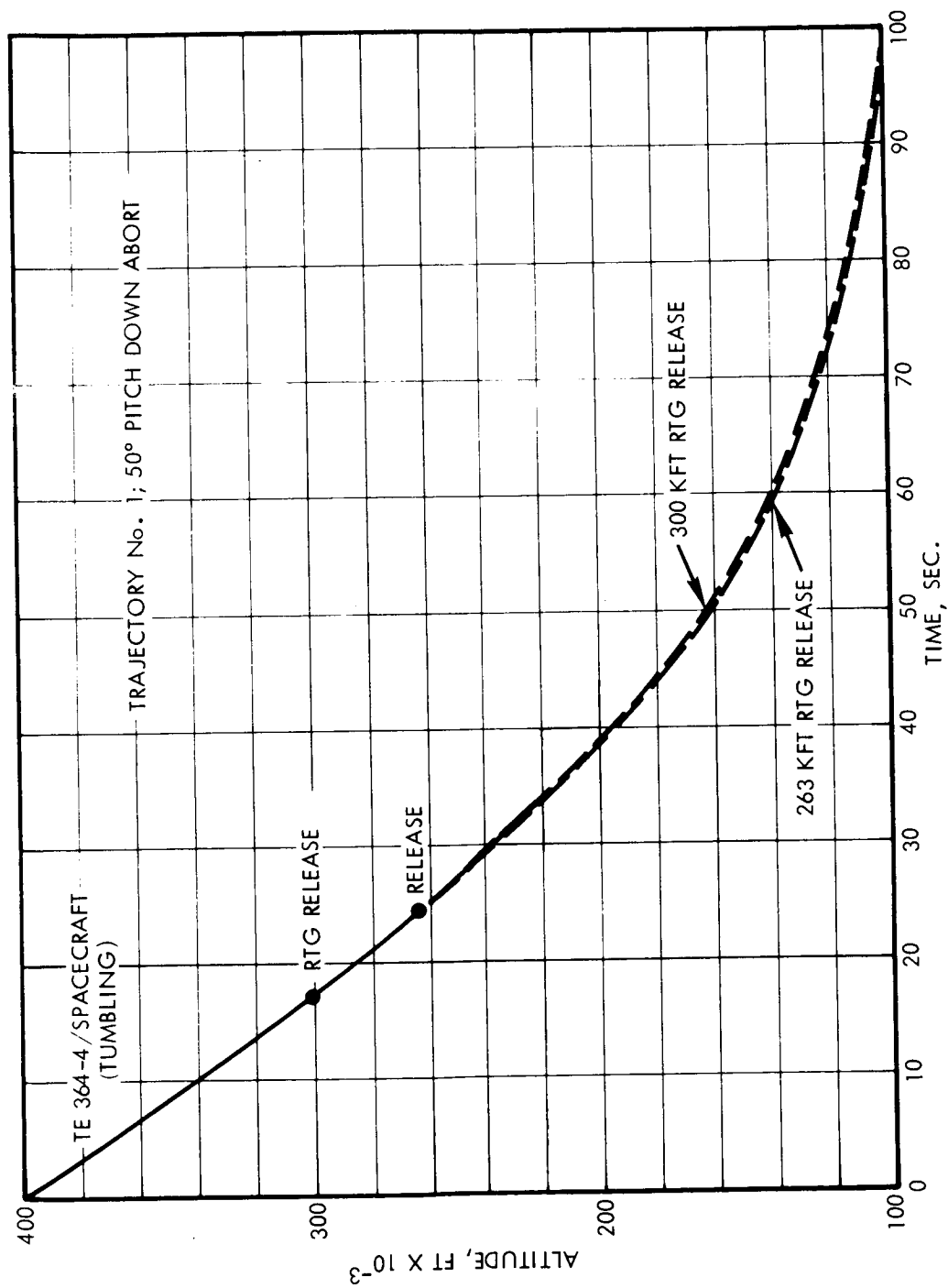


Figure 4-11. Prompt Reentry Trajectory History

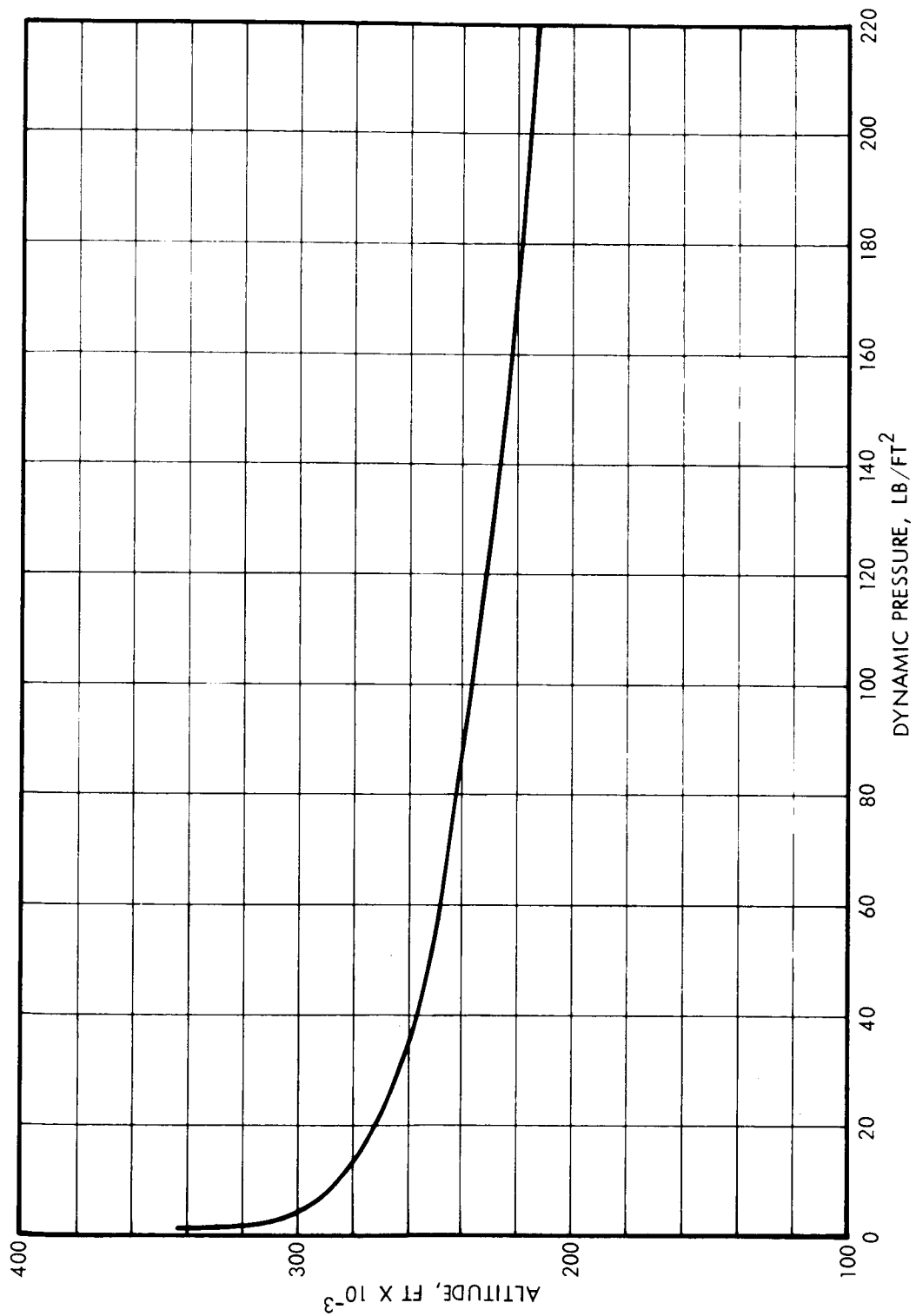


Figure 4-12, Prompt Reentry Dynamic Pressure History

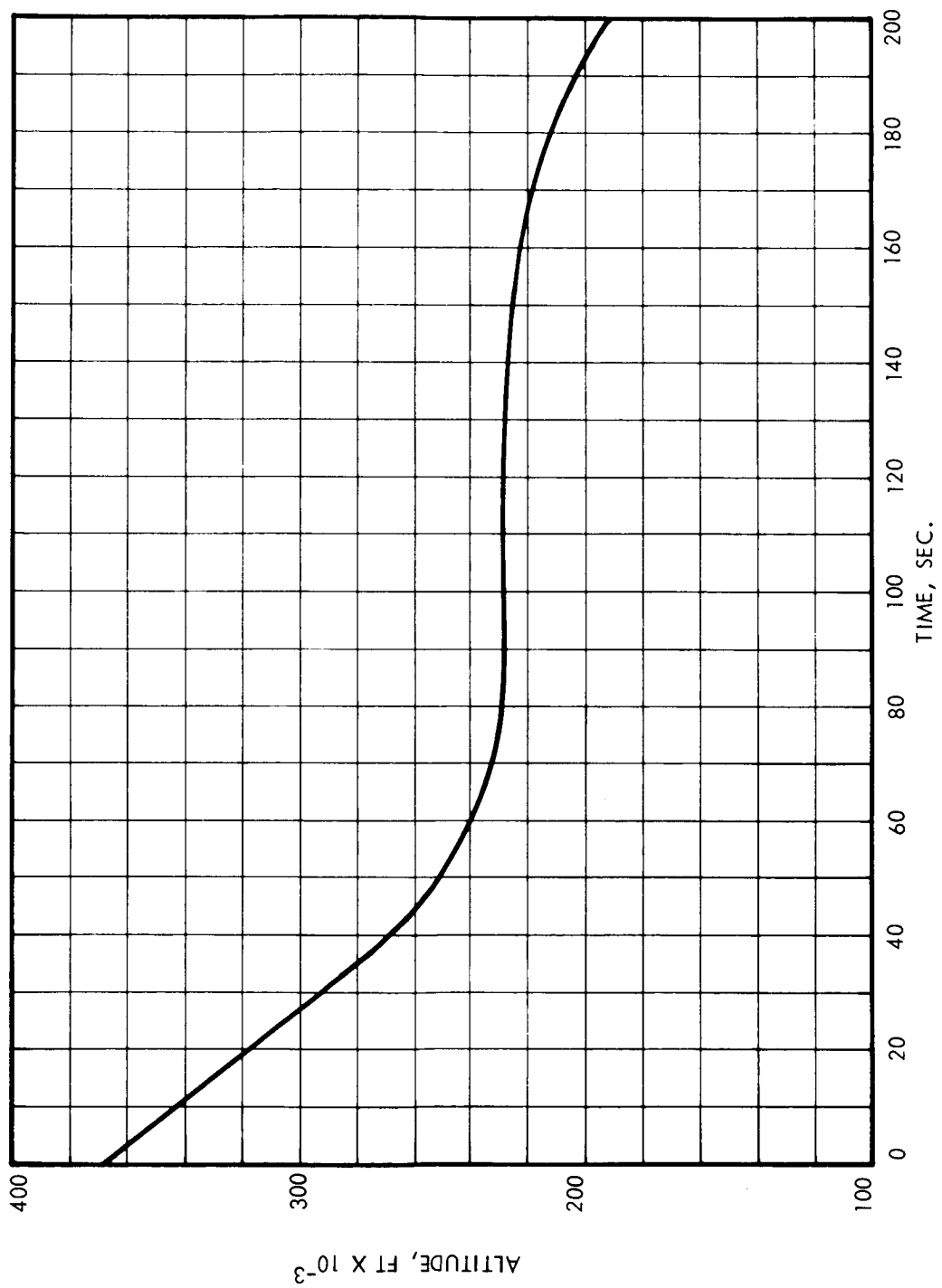


Figure 4-13. Typical Grazing Reentry Trajectory History

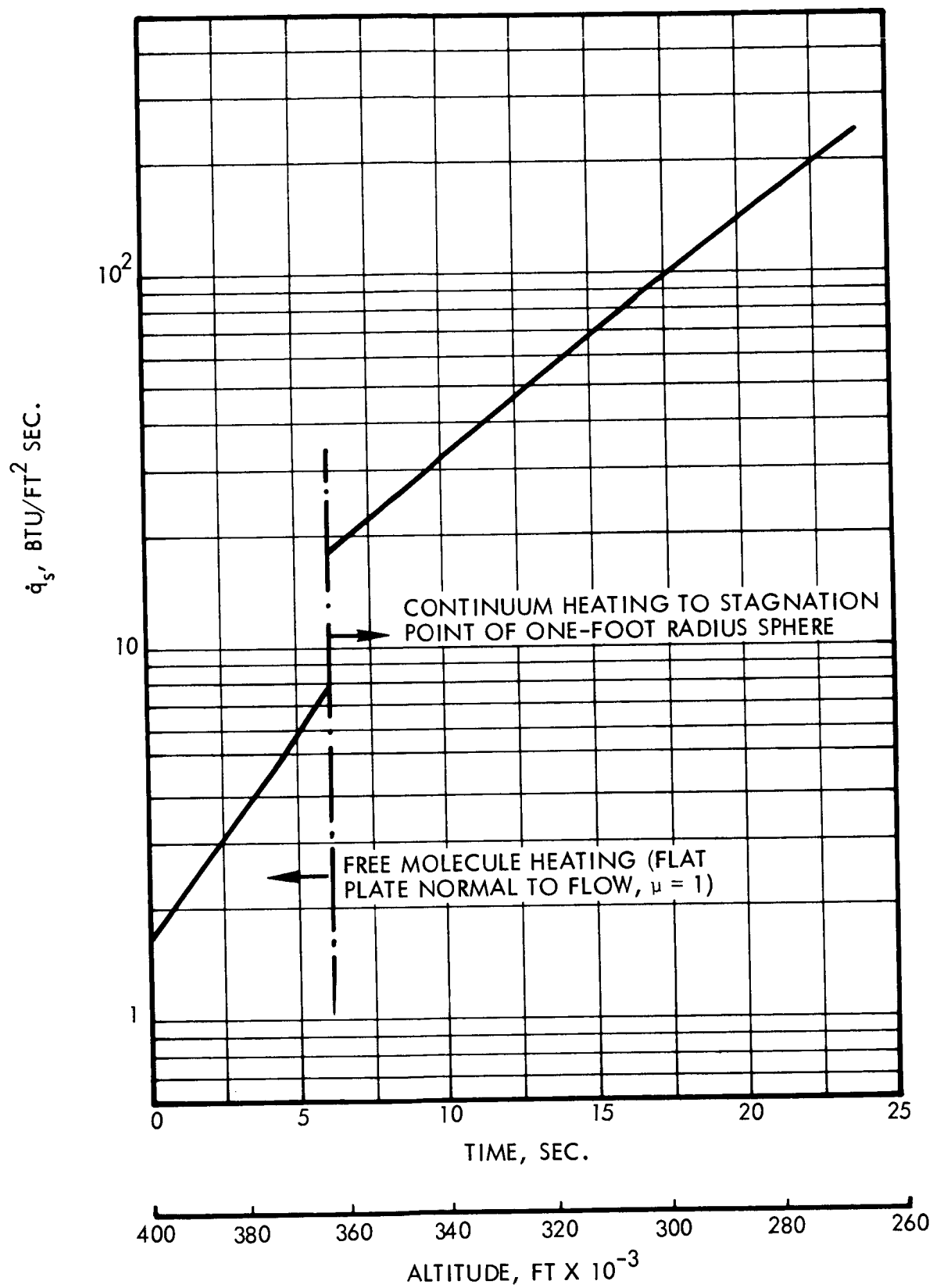


Figure 4-14. Prompt Reentry Heating Rate History
(Tumbling or Trimmed)

The transition from free molecule heating to continuum heating was assumed to occur when the free molecule heating rate was equal to the average of the continuum stagnation rates for spheres of 9 ft. and 12 ft. diameter. The heating rate shown in Figure 4-14 was multiplied by geometry factors, K_s , to account for the shape, size, and shading of individual components. The geometry factors used for the prompt reentry case are shown in Table 4-7. These geometry factors were calculated in the same manner as discussed in Section 4-1.

Table 4-7. Geometry Factors - Prompt Reentry

Motion/Flow Regime	Component		
	Reflector	RTG Support	RTG
<u>Tumbling</u>			
Free Molecule Flow	.20	.167	.145
Continuum Flow Before Reflector Failure	.10	.076	.064
Continuum Flow After Reflector Failure	-	.076	.088
<u>Trimmed ($\alpha = 180^\circ$)</u>			
Free Molecule Flow	.9	.29	.26
Continuum Flow Before Reflector Failure	.4	.128	.146
Continuum Flow After Reflector Failure	-	.156	.179

Figures 4-15 and 4-16 show the temperature histories of the Reflector and RTG Support Truss during prompt reentry, tumbling and trimmed modes, respectively. These histories were terminated at the component melt temperatures. Reradiation was verified as being negligible during the prompt reentry, therefore, Equation 4-4 was rewritten as

$$T(t) - T(o) = \frac{K_s}{\rho h C_p} \int_0^t \dot{q}_s dt \quad (4-5)$$

and this equation was utilized in determining the reentry temperatures shown in Figures 4-15 and 4-16. In both cases, the Support Truss was assumed to have an initial temperature of 325°F, which was calculated on the basis of equilibrium between conduction (from the RTGs) and reradiation heat transfer. The Reflector temperature was arbitrarily assumed to be approximately 60°F.

The RTG temperature histories are shown in Figure 4-17 up to the time of Support Truss melting. Initial RTG temperature in both cases was assumed to be 355°F, corresponding to equilibrium between conduction and reradiation. During reentry, reradiation was assumed to be negligible, and Equation 4-4 was rewritten as,

$$T(t) - T(o) = \frac{K_s A_{RTG}}{C_p W} \int_0^t \dot{q}_s dt \quad (4-6)$$

and was used to calculate the reentry temperatures shown in Figure 4-17.

Figures 4-15 and 4-16 indicate that the RTG support Truss would reach its melting point (1060°F), at altitudes of 267,000 ft. and 290,000 ft., corresponding to tumbling and trimmed reentry, respectively. The reentry dynamic pressure history shown in Figure 4-13 indicates dynamic pressures, q , at these melting altitudes of approximately 7 lb/ft² for the trimmed reentry and 25 lb/ft² for the tumbling reentry. Since these q values indicated the potential that significant loads would be imposed on the RTG Support Truss prior to melt altitude, a structural analysis of the Truss was performed to determine if structural failure could occur above the predicted melting altitude.

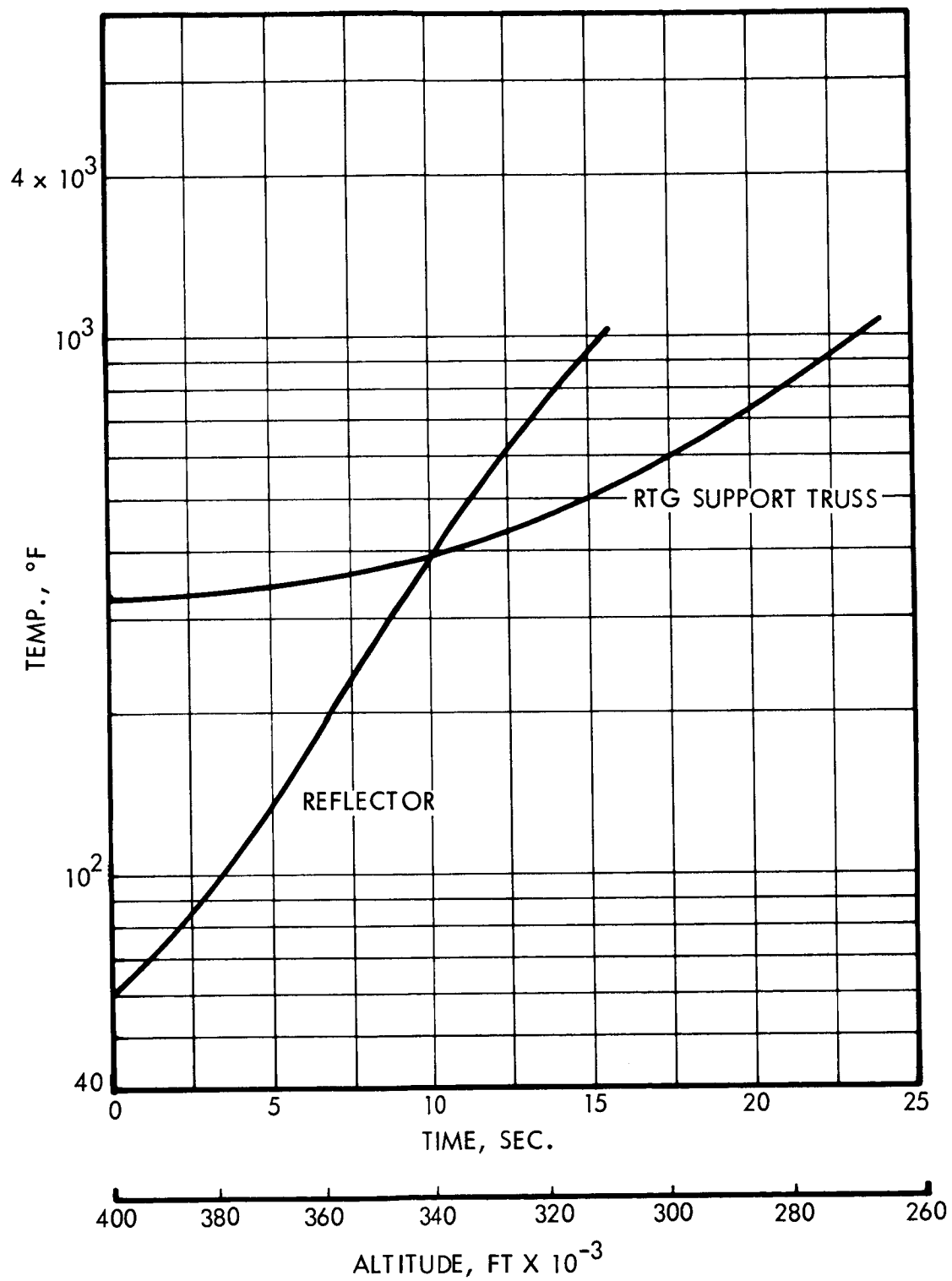


Figure 4-15. Component Temperature Histories:
Prompt Reentry, Tumbling

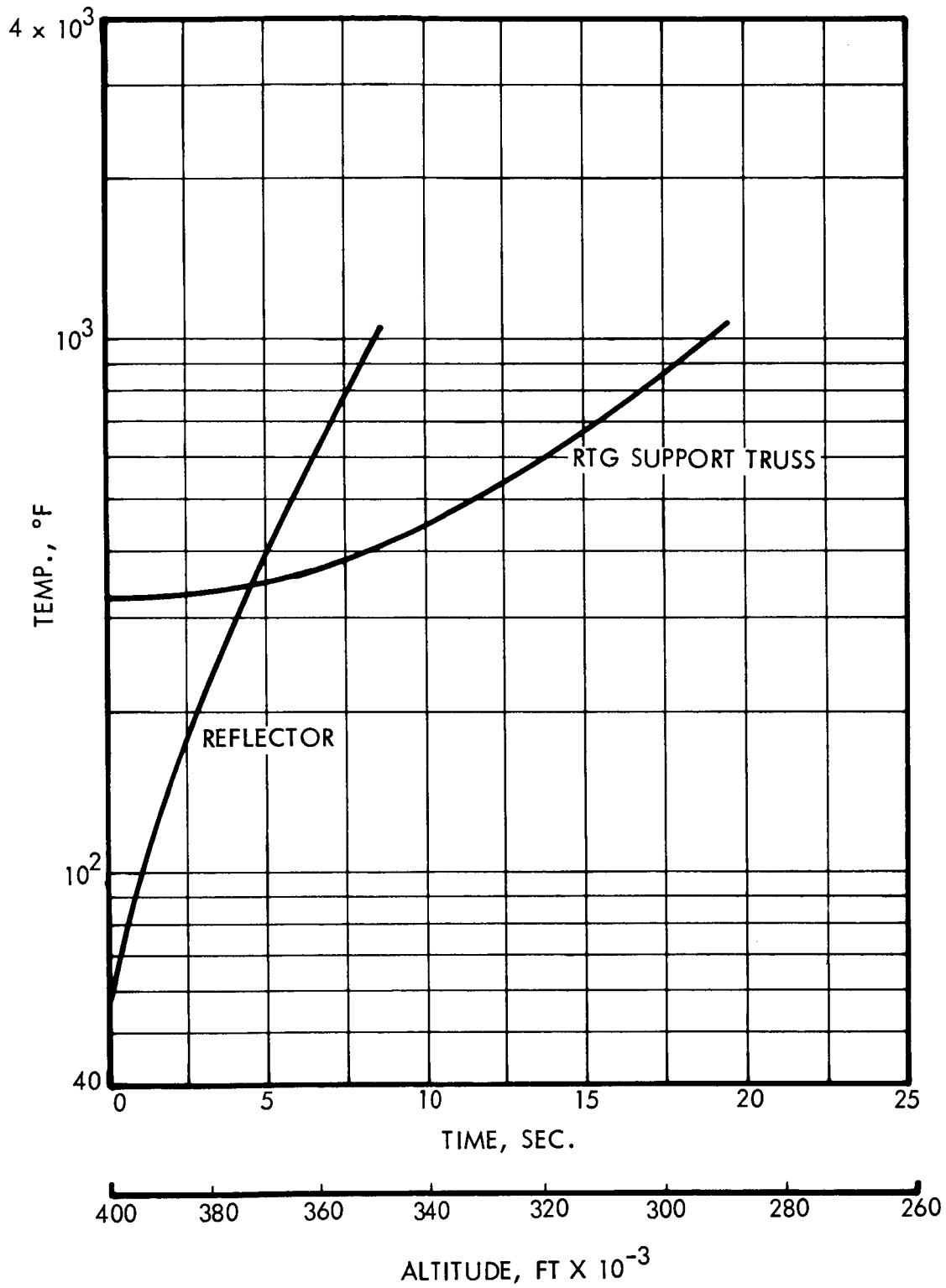


Figure 4-16. Component Temperature Histories:
Prompt Reentry, Trimmed

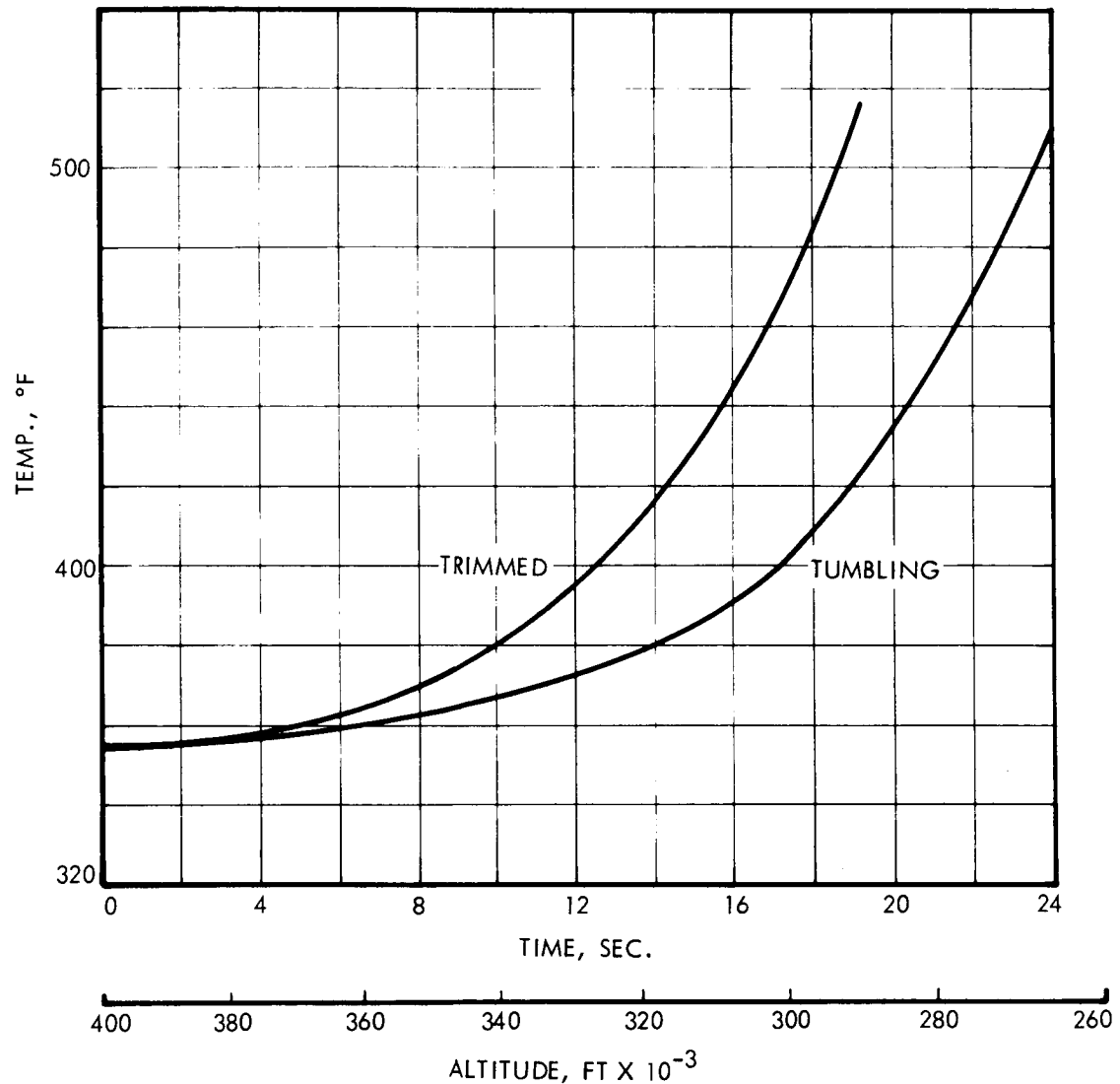


Figure 4-17. RTG Temperature History:
Prompt Reentry

The details of the structural analysis are contained in Appendix B. The analysis consisted of determining the allowable loads in the Truss legs, based on the temperature histories shown in Figures 4-15 and 4-16 and on published material properties data. These allowable load histories, represented by q_{critical} , are shown in Figure 4-18. Also shown in Figure 4-18 are the actual loads, represented by $q_{\text{trajectory}}$. As shown, failures occurred when actual loads equalled allowable loads. The results of this

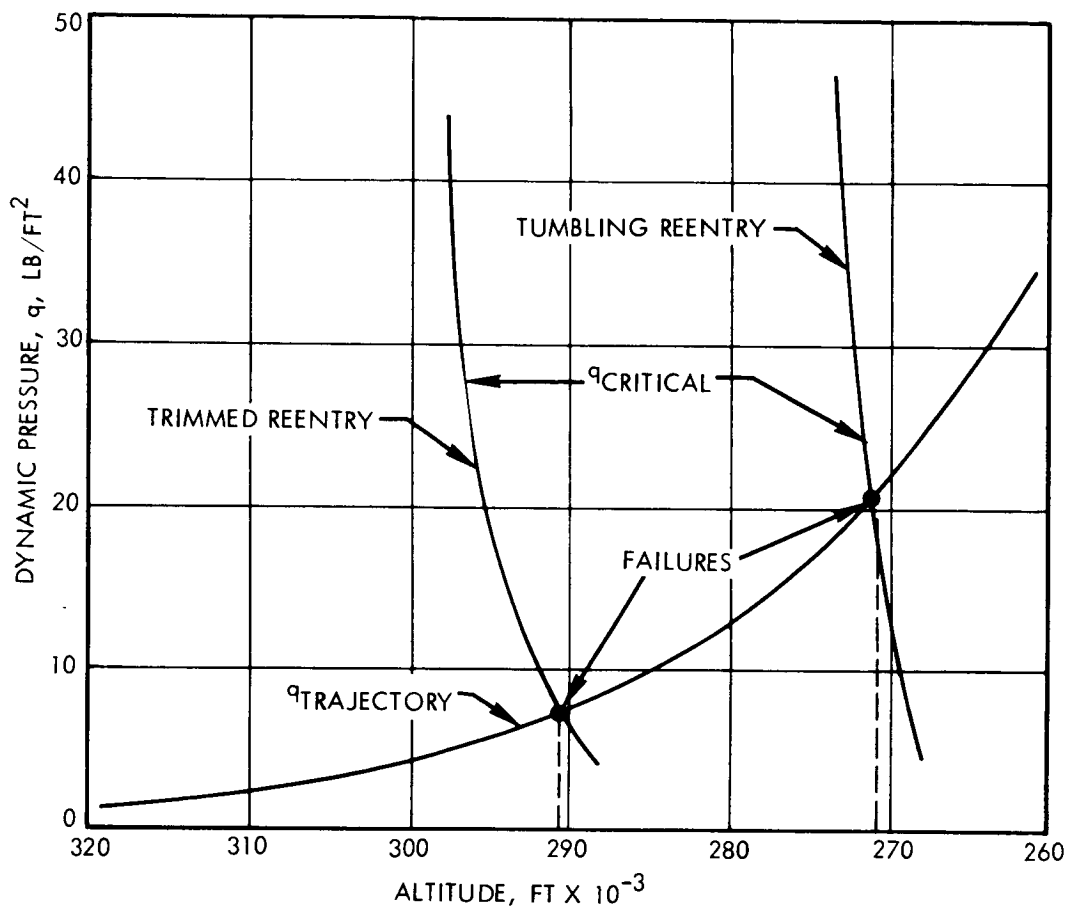


Figure 4-18. Comparison of Actual Dynamic Pressure and Critical Dynamic Pressure Required to Cause Truss Failure in Tension.

analysis indicated that the most critical failure mode was in tension, with failure occurring at approximately 291,000 ft. for the trimmed reentry and 271,000 ft. for the tumbling reentry. Although the assumptions that were made in the structural analysis were conservative i.e., would lead to higher calculated breakup altitudes, structural breakup was predicted to occur only from 1,000 ft. to 4,000 ft. above the altitudes at which melting temperatures were predicted to be reached.

In concluding the prompt reentry breakup analysis, it was necessary to verify the assumption that the spacecraft was not automatically separated from the TE 364-4 during reentry and that the RTGs remained undeployed until structural breakup. Reference to Table 4-6 indicates that reentry is initiated at 862 seconds, which, according to Reference 4-3, is 20 seconds after TE 364-4 burnout. Figures 4-15 and 4-16 indicate that the predicted breakup altitudes are reached in 19 seconds and 23 seconds after reentry is initiated, for trimmed and tumbling reentries, respectively. Therefore, breakup in neither case exceeds 43 seconds after TE 364-4 burnout. However, automatic separation of the spacecraft from the TE 364-4 does not normally occur until approximately 100 seconds after burnout (Reference 4-5), and an additional 300 seconds are required before the RTGs are normally deployed. Therefore, RTG/spacecraft breakup is predicted to occur prior to spacecraft separation or RTG deployment.

The RTG release conditions for the prompt reentry case are summarized in Table 4-8.

Table 4-8. Prompt Reentry

<u>Conditions at RTG Release</u>	<u>Tumbling</u>	<u>Trimmed</u>
Altitude	271,000 Ft.	291,000 Ft.
Latitude	15.968 ⁰ N	16.156 ⁰ N
Longitude	34.552 ⁰ W	34.971 ⁰ W
Inertial Velocity	42,563 Ft./Sec.	42,698 Ft./Sec.
Inertial Flight Path Angle	6.654 ⁰ (Down)	6.946 ⁰ (Down)
Inertial Azimuth	114.187 ⁰	114.070 ⁰
RTG Temperature	490 ⁰ F	510 ⁰ F
Time from TE 364-4 Burnout	43 Sec.	39 Sec.

5. PROPELLANT TANK FAILURE ANALYSIS

A preliminary analysis was conducted to determine the response of the spacecraft propellant tank to the potential environments imposed by launch pad or high altitude aborts, and the environments subsequently imposed on the RTGs by propellant tank failure.

5.1 LAUNCH PAD ABORT

A launch pad abort of the Atlas/Centaur/TE 364-4 vehicle may result in exposure of the spacecraft propellant tank to overpressure and shrapnel. In the event of a launch pad abort, each of the three stages were conservatively estimated to produce an overpressure equivalent to that which would be produced by a charge of TNT in the amount of 20 percent of the propellant weight. The peak reflected overpressures, undamped by any intervening structure between the explosion source and spacecraft tank, were first calculated according to the method of References 5-1 and 5-2. It was assumed that the explosion was initiated at the centroid of the propellant masses of each of the stages. These overpressures, with no blockage, are shown in Table 5-1. Calculation of the reduction in

Table 5-1. Overpressures at Spacecraft
Propellant Tank Due to Launch
Pad Abort

<u>Stage</u>	<u>Overpressure from 20% TNT Equiv.</u>	
	<u>Without Blockage</u>	<u>With Blockage</u>
Atlas	1187	201
Centaur	2062	325
TE 364-4	8834	1680

overpressure of a shock wave due to structural blockage represents an extremely difficult gas dynamics problem. The many variables include the effect of partial or total blockage, collision and mixing of deflected shock waves, the effect of moving shrapnel on the shock wave, and the energy lost in deforming and moving pieces of structure. Calculations previously performed by TRW for the Transit spacecraft have indicated

that the overpressures may be reduced by as much as a factor of ten due to structural blockage.

As an approximation of the effects of structural blockage, the analysis assumed that the damped peak reflected overpressures at the spacecraft tank were equal to the undamped peak static overpressures predicted by the methods of Reference 5-2. This assumption effectively yields blockage factors between 5 and 7. Although it could reasonably be expected that the blockage factor, for example, for the Atlas explosion would be greater than for the TE 364-4 explosion, due to the complete blockage presented by the Centaur stage, it was subsequently found that the likelihood of spacecraft tank failure was not significantly affected by the selection of blockage factor. The damped, peak reflected overpressures at the spacecraft tank are shown in Table 5-1.

The spacecraft propellant tank is a 16.5 inch diameter sphere which is supported at its equator by three equally spaced bipod trusses. The tank is a welded structure which is fabricated from two 0.030 inch thick forged titanium alloy (Ti-6Al-4V) hemispheres. The propellant is liquid hydrazine and is pressurized by nitrogen gas separated by a diaphragm. The tank is pressurized to approximately 535 psig at launch, and the external static pressure must be 79 psi greater than the internal pressure to cause buckling. With the conservative assumption that the buckling pressure due to a pressure wave is equal to the static buckling pressure, it can be seen from Table 5-1 that a failure of the propellant tank will occur only in the case of a TE 364-4 abort at launch. It was subsequently calculated that for the assumed blockage factor, as low as 3 percent yield of the TE 364-4 would cause tank rupture.

In addition to the overpressure created during a launch pad abort, shrapnel may be created by the exploding stages. No estimates of the resultant fragment sizes and velocities were made, neither were the shrapnel characteristics necessary to cause tank failure calculated. Rather, it was assumed that a piece of shrapnel could be generated during a launch pad abort which would cause tank failure, and that the environment resulting from shrapnel-induced tank failure would be the same as overpressure-induced failure.

The contribution of the hydrazine propellant to the energy released

from the tank at rupture was assessed. However, from Reference 5-3 and from informal discussion with Sandia personnel, it was concluded that the hydrazine would not contribute to the energy release. Therefore, the overpressure resulting from tank failure was calculated on the basis of only the pressurized nitrogen. In this case the resulting energy release corresponded to an explosion of 0.18 pounds of TNT. The overpressure at the location of the inboard RTG due to a failure of the propellant tank at launch was calculated to be 50 psig, based on an assumed blockage factor of 4.0. This relatively low value of blockage factor appears reasonable, since there is little blockage afforded by the electronic components between the tank and the inboard RTGs. Figure 5-1 is a top view of the spacecraft platform, and shows the location of the propellant tank, inboard RTGs in the launch configuration, and intervening structures. It was assumed that the tank would separate into two hemispheres, and that all equipment between the tank and the RTGs would be broken loose by the overpressure wave from the tank failure. One of the tank fragments and the intervening equipment would then be accelerated, intact, into one of the inboard RTGs. The components which may be affected are the Power Inverters, Command Distribution Unit (CDU), Conscan and Control Electronics Assembly (CEA), and the RTG Slack Boxes. The side panels will be blown apart and the fragments will probably impact the RTGs. The weights and calculated velocities of these shrapnel are presented in Table 5-2. The velocities were computed by using the method presented in Reference 5-4.

Table 5-2. Shrapnel Characteristics at
Inboard RTGs Due to Spacecraft Tank
Rupture

<u>Description</u>	<u>Weight</u>	<u>Velocity (ft/sec)</u>
Tank Hemisphere	2.1	339
Power Inverter	12.0	7
Command Distribution Unit	10.0	17
or		
Conscan and Control Electronics Assy.	7.8	22
RTG Slack Box	2.0	31
Side Panel	1.5 (Total)	231

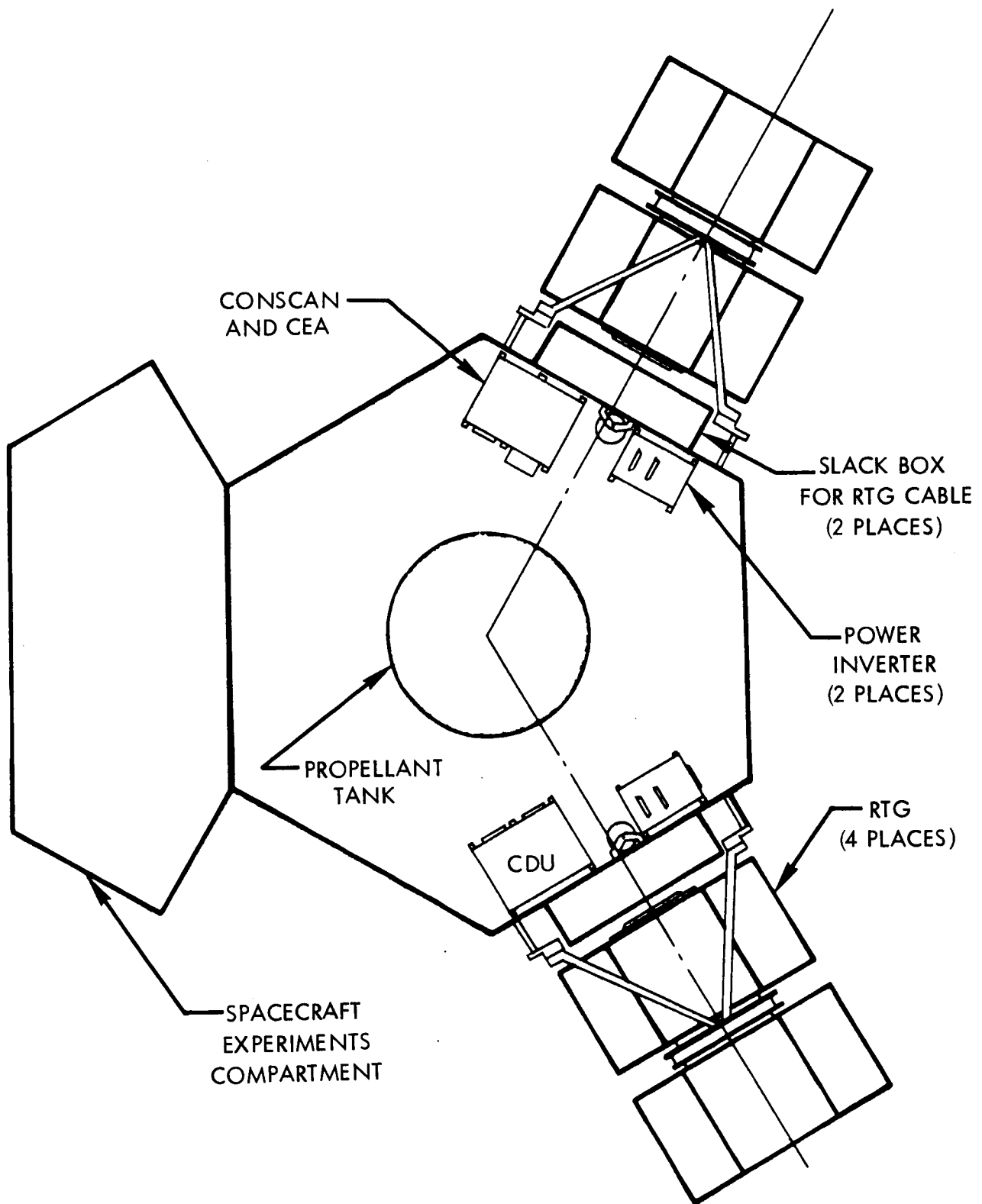


Figure 5-1. Top View of Spacecraft Platform
(Reflector Removed)

5.2 HIGH ALTITUDE ABORT

The overpressures and shrapnel caused by a spacecraft tank failure at high altitude (i.e. vacuum) were investigated utilizing the approach discussed in Section 5.1. Potential causes of tank failure included the overpressure and shrapnel from an explosion of the TE 364-4 motor.

The overpressure resulting from a 20 percent TNT equivalent yield of the TE 364-4 motor was calculated according to the analytical method which is presented in Reference 5-5. The resultant overpressure was found to be negligibly small. However, it was assumed that the shrapnel which would be generated by the explosion could cause spacecraft tank rupture, which in turn could cause overpressure and shrapnel at the RTG locations.

The overpressure at the RTG locations was also found to be negligibly small, according to the method of Reference 5-5. However, tank rupture could result in a hemispherical piece of the propellant tank being impacted into one of the inboard RTGs at 366 ft/sec, assuming that this piece is negligibly affected by the side panel or slack box. This velocity is greater than the velocity resulting from a launch pad abort because the tank pressure increases after liftoff to 640 psig, due to an increase in tank temperature. Because the overpressure wave is rapidly dissipated in the vacuum environment, the equipment between the tank and RTGs are not expected to be dislodged to form shrapnel.

6. REFERENCES

- 4-1 Flight Performance Handbook for Powered Flight Operations, Edited by J. F. White, STL, March, 1962.
- 4-2 "Deceleration and Heating of a Body Entering a Planetary Atmosphere from Space," Carl Gozley Jr., Rand Report, p-955, 18 February, 1957.
- 4-3 Pioneer F RTG Safety Analysis/Nominal Ascent Trajectory Simulations, General Dynamics/Convair, 28 April, 1970.
- 4-4 TRW IOC 67-3324.2-22, "Reentry Debris Hazards Study - Thermal Survivability Analysis," T. L. Rivell and R. L. Bacharach, 20 February 1967.
- 4-5 "Pioneer F AEC Safety Study; Phase I; Launch Vehicle Hardware, Launch Complex, and Trajectory Data," General Dynamics, Convair Division, GDC-BTD-70-010," Preliminary Copy, 30 June 1970.
- 4-6 TRW IOC 67-3324.2-65, "Reentry Debris Hazards Study - Structural Temperature Histories," T. L. Rivell and R. L. Bacharach, 31 March 1967.
- 4-7 Telecon between J. M. Bell, TRW Systems, and L. Keller, Sandia Corp., July 1970.
- 5-1 A Calculation of the Blast Wave from a Spherical Charge TNT, by H. L. Brode, Rand Corp. Report P975, 26 May 1958.
- 5-2 Information Summary of Blast Patterns in Tunnels and Chambers, BRL Report No. 1390, Aberdeen Proving Grounds, March 1962.
- 5-3 Stability Tests of Monopropellants Exposed to Flames and Rifle Fire, by G. S. Glatts, Jet Propulsion Laboratory Technical Report No. 32-172, 26 February 1962.
- 5-4 The Gurney Formula and Related Approximations for the High-Explosive Deployment of Fragments, by I. G. Henry, Hughes Aircraft Co. Report No. PUB-189, April 1967.
- 5-5 On Explosion in Vacuo, By C. K. Thornhill, A.R.D.E. Report (B) 30/58, 30 January, 1959

APPENDIX A NOMENCLATURE

A	=	Area
C_D	=	Drag Coefficient
C_p	=	Specific heat
h	=	Thickness
H_e	=	Stagnation enthalpy at edge of boundary layer
H_{ws}	=	Stagnation enthalpy at stagnation point (at the wall)
K_R	=	Radiation shape factor (average radiation heat transfer rate from surface/radiation heat transfer rate from unshaded surface)
K_S	=	Geometry factor (average convective heat transfer rate/stagnation point heat transfer rate to standard body)
\dot{q}_D	=	Thermal dissipation rate from RTG
\dot{q}_R	=	Radiation heat transfer rate
\dot{q}_S	=	Stagnation point convective heat transfer rate
T	=	Temperature
T_f	=	Temperature at failure
T_i	=	Initial temperature
t	=	Time
V_a	=	Velocity relative to atmosphere
W	=	Weight
α	=	Angle of attack
β	=	Ballistic coefficient ($W/C_D A$)
μ	=	Thermal accommodation coefficient
ρ	=	Density
ρ_∞	=	Ambient atmospheric density
σ	=	Stefan-Boltzmann constant (0.476×10^{-12} BTU/ft ² -sec°R ⁴)

APPENDIX B STRUCTURAL ANALYSIS

B1. INTRODUCTION

This Appendix describes the analyses performed to assess the effect of considering reentry loads in determining the altitude at which the Pioneer RTG Support Truss would fail when subjected to the re-entry heating environment. The conditions analyzed were for the prompt, shallow angle reentry in both a random tumble and trimmed orientation.

The previous thermal analyses had indicated that for the prompt reentry the Support Truss would reach the melting point (1060°F) at an altitude of 290,000 feet for a trimmed spacecraft, or 267,000 feet if the spacecraft was tumbling. The reentry dynamic pressure (q) history gave maximum q values at these melting altitudes of approximately 7 psf for the trimmed condition and 25 psf for the tumbling vehicle. Since these q values indicated that potentially significant loads would be imposed on the spacecraft, a brief, conservative structural analysis was required in order to determine if the structural failure altitude could occur above the melting altitude.

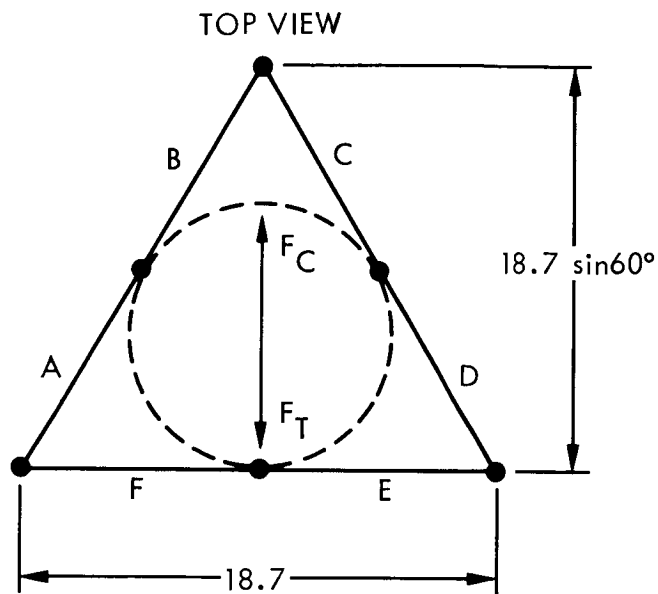
B2. ANALYSIS

As previously indicated, the purpose of this analysis was to determine an upper altitude for breakup. Therefore, several conservative assumptions were made, including the following:

- o The worst spacecraft orientation is that which causes all of the RTG load to be reacted by only two of the truss legs (e.g. legs B and C of Figure B-1). This orientation was assumed to be possible for the conditions which could produce either tension or compression in the two legs.
- o Any shielding effects were neglected. Thus, the leg temperatures were independent of orientation, and both RTG and spacecraft aerodynamics were unaffected by interaction effects.
- o Rotational accelerations at the altitudes of interest were considered small enough to be neglected.

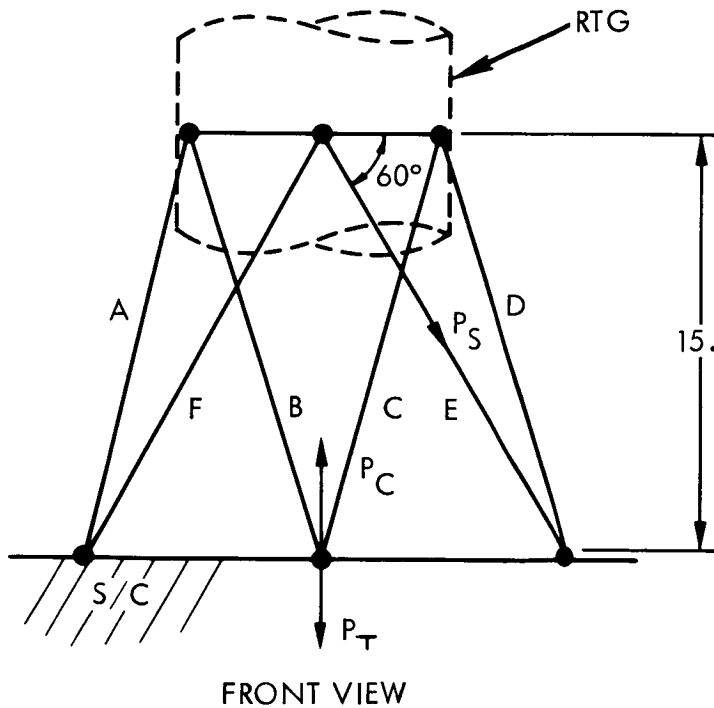
B2.1 Actual Truss Loads

The analysis considered both a compression (Euler buckling) and an axial, tensile failure mode for the small aluminum (2024-T351) I-beams which constitute the legs of the truss. The equations for determining the



F_c = RTG LOAD PRODUCING
COMPRESSION IN LEGS
B AND C.

F_T = RTG LOAD PRODUCING
TENSION IN LEGS B
AND C.



P_c = TENSION LOAD

P_c = COMPRESSION LOAD

P_s = AXIAL LOAD IN LEG

Figure B-1. Idealized RTG Support Truss Geometry

load in the two legs of the truss were determined as follows:

$$\begin{aligned} N_{sc} &= \text{Spacecraft Deceleration (g's)} \\ &= \frac{(C_D A)_{sc} q}{W_{sc}} \\ &= \frac{q}{\beta_{sc}} \end{aligned}$$

$$\begin{aligned} F_I &= \text{Inertial force on RTG (Lbs)} \\ &= N_{sc} W_{RTG} \\ &= \frac{q}{\beta_{sc}} W_{RTG} \end{aligned}$$

$$\begin{aligned} F_A &= \text{Aerodynamic force on RTG (Lbs)} \\ &= (C_D A)_{RTG} q \\ &= \frac{q}{\beta_{RTG}} W_{RTG} \end{aligned}$$

$$\begin{aligned} F &= \text{Total net load on RTG (Lbs)} (\text{can be applied forward or backward depending on orientation - consider both possibilities}) \\ &= \pm (F_A - F_I) \\ &= \pm q W_{RTG} \left(\frac{1}{\beta_{RTG}} - \frac{1}{\beta_{sc}} \right) \\ M &= \text{moment at base of leg due to RTG load } F \text{ (in-lb.)} \\ &= 15F \end{aligned}$$

To find the vertical force (P) at the lower end of legs B and C,

$$\begin{aligned} M &= P \times 18.7 \sin 60^\circ \\ &= P \times 18.7(.866) = 16.2 P \\ 15F &= 16.2 P \\ P &= .926 F \end{aligned}$$

P_s = axial force in each of legs B and C

$$\begin{aligned} 2P_s (\sin 60^\circ) &= P \\ P &= 2 P_s (.866) = 1.732 P_s \end{aligned}$$

$$1.732 P_s = .926 F$$

$$P_s = .534 F$$

Substituting in Equation B-1

$$P_s = \pm .534 \left[W_{RTG} \left(\frac{1}{\beta_{RTG}} - \frac{1}{\beta_{SC}} \right) \right] q \quad (B-2)$$

The actual load in each of the legs, as a function of the reentry q , was then determined by substituting the appropriate data from Table B-1 into the above equation.

Table B-1. Structural Analysis Assumptions

<u>Weights</u>		
RTG System	60.0 lb each pair	
<u>Ballistic Coefficients</u>	$\beta = \frac{W}{C_D A}$	
Spacecraft - prompt reentry, tumbling	$\beta = 8.8$	
Spacecraft - prompt reentry, trimmed	$\beta = 6.1$	
RTG	$\beta = 40$	

B2.1.1 Spacecraft-Tumbling

$$\begin{aligned} P_s &= \pm .534 \left[60 \left(\frac{1}{40} - \frac{1}{8.8} \right) \right] q = \pm .534 [1.5 - 6.82] q \\ &= \pm 2.84 q \\ q &= \pm 0.352 P_s \end{aligned} \quad (B-3)$$

B2.1.2 Spacecraft-Trimmed

$$\begin{aligned} P_s &= \pm .534 \left[60 \left(\frac{1}{40} - \frac{1}{6.1} \right) \right] q = \pm .534 [1.5 - 9.84] q \\ &= 4.45 q \\ q &= 0.224 P_s \end{aligned} \quad (B-4)$$

B2.2 Truss Allowable Load

The allowable compressive stress for one leg of the truss is a function of the modulus of elasticity (E) and the effective slenderness ratio (L'/ρ). L' is an effective length which accounts for end fixity

conditions and for this case is

$$L' = .7L = .7 \frac{(15)}{\sin 60^\circ}$$

$$= 12.11 \text{ in.}$$

From the section properties the minimum radius of gyration (ρ_{\min}) for the truss leg is:

$$\rho_{\min} = .1839 \text{ in.}$$

$$\text{Then } \frac{L'}{\rho} = \frac{12.11}{.1839} = 66$$

The allowable room temperature compressive stress for 2024-T351 Aluminum with $L'/\rho = 66$ was taken from curve #9 in the Northrup Structural Design Manual, Figure 302.2-5 and is

$$F_c = 22,600 \text{ psi @ room temperature}$$

The allowable room temperature tensile stress (F_{t_u}) in the truss leg was obtained from MIL Handbook 5. This value is

$$F_{t_u} = 66,000 \text{ psi}$$

The effects of elevated temperature on the allowable loads were also determined from the data in MIL Handbook 5. Figures 3.2.3.1.4 and 3.2.3.2.1 (a) of this handbook present the effect of elevated temperature on E_c and F_{t_u} respectively. The allowable loads were then determined by multiplying these allowable stresses by the area (.1145 in²) of the truss. The results are shown in Table B-2.

Table B-2. Truss Allowable Loads

T °F	%E	%F _{t_u}	Compression		Tension	
			F _c psi	P _s Allow lb.	F _{t_u} psi	P _s Allow lb.
Room	100	100	22600	2585	66,000	7560
600	70	25	15810	1810	16,500	1890
700	61	15	13790	1580	9,900	1133
*800	≈40	≈6	9050	1037	3,960	453
*900	≈24	≈2	5420	621	1,320	151
*1000	≈9	≈.3	2030	232	198	22.6

*Extrapolation

B2.3 Determination of Structural Failure

Either tension or buckling (compression) failure will occur when,

$$P_s = P_{s_{\text{Allow}}}$$

B2.3.1 Spacecraft-Tumbling

Values of critical dynamic pressure were computed for both tension and compression using Table B-2 and Equation B-3. These results are shown in Table B-3.

Table B-3. Tumbling Loads

<u>Temp.</u>	<u>Alt.</u>	<u>q_{cr} Tens</u>	<u>q_{cr} comp</u>	<u>q_{actual}</u>
600 F	299,000	665	637	4.4
700 F	289,000	399	556	7.6
800 F	281,000	159	364	12.
900 F	274,000	53.1	218	16.7
1000 F	269,000	7.9	81.6	22.6

Also shown in Table B-3 are the actual loads. From Table B-3, it is evident that tension failure will occur prior to compression failure. This is also shown in Figure B-2, where tension failure is seen to occur at approximately 271,000 ft.

B2.3.2 Spacecraft-Trimmed

Values of critical dynamic pressure were computed using Table B-2 and Equation B-4. The results are shown in Table B-4, where it is again evident that failure will occur due to tension. These results are shown in Figure B-2, where failure occurs at approximately 291,000 feet.

Table B-4. Trimmed Loads

<u>Temp.</u>	<u>Alt.</u>	<u>q_{cr} Tens</u>	<u>q_{cr} comp</u>	<u>q_{actual}</u>
600 F	319,000	424	405	1.4
700 F	310,000	254	354	2.3
800 F	302,000	101	232	3.6
900 F	297,000	38.8	139	5.0
1000 F	289,000	5.0	52.	7.6

